WEST VIRGINIA UNIVERSITY

PLASMA PHYSICS GROUP

INTERNAL REPORT PL-050

Zeeman Splitting for LIF Transitions and
De-convolution Technique to Extract Ion Temperature

Ar II 611.49 nm
Ar II 664.37 nm
Ar II 668.43 nm

He I 587.57 nm

R.F. Boivin

December 2001

1.0 THEORY OF ZEEMAN SPLITTING

The interaction of the magnetic moment of an atom with an applied magnetic field results in the splitting of the observed spectral lines. For all lines that are not singlets, the so-called anomalous Zeeman effect is observed. It consists of a splitting into many components with separations that are rational multiples of the normal splitting. The number of energy levels obtained in a magnetic field depends upon the total angular momentum value and is given by $(2J+1)$. The energy difference introduced by the interaction of the magnetic moment and the magnetic field B is given by [Marr]:

$$DE = e\,h\,(4\pi m_e)^{-1}\,B\,g_j M_j = b\,B\,g_j M_j \qquad (1.1)$$

where $b = eh/(4\pi m_e) = 9.274 \times 10^{-24}$ Joule Tesla^{-1} is the Bohr magneton, M_j is the magnetic orbital quantum number, and g_j is the Landé factor which differ from level to level. The Landé factors depend on the values of the quantum numbers L (orbital angular momentum), S (angular momentum) and J (total angular momentum) and are given by [Herzberg]:

$$g_j = 1 + [\,\{J(J+1) + S(S+1) - L(L+1)\} / \; 2J(J+1)\,] \qquad (1.2)$$

Considering two split levels (level 1 and 2) the energy associated with the different possible transitions is from equation (1.1) given by:

$$DE = b\,B\,(g_1 M_1 - g_2 M_2) \qquad (1.3)$$

The interaction of the magnetic moment with the magnetic field causes all the terms to split into energy levels with the same spacing since the magnetic orbital quantum number M_j changes only by unity and transitions between one state and another are governed by the normal selection rule:

$$DM_j = 0 \text{ or } \pm 1 \qquad (1.4a)$$

with: $$M_j = J, J\text{-}1, J\text{-}2 \ldots\ldots -J \qquad (1.4b)$$

Transitions for $DM_j = 0$ are called the p components, while transitions with $DM_j = \pm 1$ are identified as the s components. In weak to moderate magnetic fields, both p and s components are arranged symmetrically about the zero-field frequency with the p components being generally less displaced than the s components. Re-writing equation (1.3) in terms of wavelength (and frequency), the different components p $(M_1 = M_2)$ and s $(M_1 - M_2 = \pm 1)$ of the transition are given by:

$$Dl = b\,l^2\,B\,c^{-1}\,h^{-1}\,(g_1 M_1 - g_2 M_2) \qquad (1.5a)$$

$$Dn = b\,B\,h^{-1}\,(g_1 M_1 - g_2 M_2) \qquad (1.5b)$$

1.1 INTENSITIES OF THE ZEEMAN COMPONENTS

There are three different scenarios regarding the value of the total angular momentum for a given transition: $J \rightarrow J$, $J \rightarrow J + 1$ and $J \rightarrow J - 1$. The intensities of all Zeeman components for a $J \rightarrow J$ transition are given by the expressions [Marr]:

$M \rightarrow M$	(p components)	$I_p = 4KM^2$	(1.6a)
$M \rightarrow M \pm 1$	(σ components)	$I_s = K\,(J \pm M + 1)\,(J \text{ -/+ } M)$	(1.6b)

The intensities of all Zeeman components for a $J \rightarrow J + 1$ transition are given by the expressions [Marr]:

$M \rightarrow M$	(p components)	$I_p = 4K\,(J + M + 1)\,(J - M + 1)$	(1.7a)
$M \rightarrow M \pm 1$	(σ components)	$I_s = K\,(J \pm M + 1)\,(J \pm M + 2)$	(1.7b)

Since the initial and final states can be interchanged the intensities for a $J \rightarrow J - 1$ are given by the expression (1.7a and 1.7b). K is a constant related to the initial line intensity. The total intensity of all Zeeman components is given by:

$$P = \mathring{a}_{M'M''} I_p + \mathring{a}_{M'M''} I_s \qquad (1.8)$$

The statistical weight of any given Zeeman components is thus:

$$w = \tfrac{1}{2} I_p / P \quad \text{or} \quad \tfrac{1}{2} I_s / P \quad ; \qquad (1.9)$$

the ½ factor being related to the symmetry of the Zeeman pattern.

1.2 ZEEMAN " BROADENING "

We will now consider that the fluorescence linewidth is the convolution of Doppler broadening and Zeeman broadening (splitting). The other broadening mechanisms (Stark, Instrumental, Power and Natural) have negligible contributions to the resulting lineshape (for more information see Internal Report WVU-PL-039).

In reality, there is no such thing as a Zeeman broadening. Instead, each component of the observed Zeeman splitting is broadened by thermal motion (Doppler broadening). Thus, the resulting lineshape can be best described as the envelope that encompasses all of the different Doppler broadened Zeeman components. The exact de-convolution technique is presented in section 1.3.

When the magnetic field intensity is small, the Zeeman splitting can be approximated by an equivalent broadening (valid only when $Dl_{Zeeman} << Dl_{Doppler}$). In all cases, this simple approach will slightly overestimate the Zeeman correction, resulting in ion temperature slightly lower than the real ion temperature (see example in section 4.3). Thus, this first approximation technique is useful for a quick evaluation of T_i and to validate the more elaborate de-convolution technique presented in section 1.3.

1.2.1 First Order Approximation

As seen in section 1.0, the different p components are symmetrically distributed around the central unshifted line. According to the respective statistical weights derived in section 1.1, the distribution of the different components can be roughly described as a Normal (or Gaussian) distribution. The wavelength distribution function can be expressed as:

$$F(l) = \frac{1}{\sqrt{2p}\, s} \exp\left[\frac{-(l - m_l)^2}{2s^2}\right] \tag{1.10}$$

where m_λ is the average and s^2 is the variance of the Normal distribution, respectively. The variance for the Normal distribution (discrete values) is given by:

$$s^2 = \sum_i (l_i - m_l)^2 / n \tag{1.11}$$

where l_i is a Zeeman component wavelength and m_l is in this case the central wavelength. The summation takes in account the statistical weight of each Zeeman component. From this variance we can obtain the FWHM given by the expression:

$$FWHM = D l_{Zp} = 2\,(2 \ln 2)^{1/2}\, s \tag{1.12}$$

The FWHM is the corresponding Zeeman broadening for the p components.

For the s components, the situation is different. Two line clusters are symmetrically shifted on each side of the central line. In particular, each line cluster distribution is asymmetric. Each cluster has either the most intense line closest or farthest to the central wavelength. Although the situation is different from the p components, we will as a first approximation, the same approach to calculate the resulting Zeeman broadening. First, we calculate the average wavelength of each cluster as:

$$m_l = \sum_i l_i / n \ , \tag{1.13}$$

where m_l corresponds to the average shift of the s components (Zeeman shift) with respect to the unshifted central wavelength. We now use equations (1.11) and (1.12) to calculate the FWHM of a particular s cluster. Because of the asymmetry of the cluster, we can suppose that the real $D l_s$ is probably a bit larger (about the same as the p broadening). As seen in equation (1.5) the Zeeman Broadening is directly proportional to the magnetic field intensity. Thus, both p and s components can be extrapolated for different magnetic field values from a single calculation of the broadening.

1.2.2 Ion Temperature from the Resulting Lineshape

In this section, we describe the technique used to obtain the ion temperature from the resulting fluorescence lineshape. There are a number of advantages to using frequency units

instead of wavelength: frequency is independent of the air refractive index and is the same in air and vacuum. The conversion between frequency and wavelength is simply $n = c/l$ which in terms of bandwidth becomes, $Dn = c\, Dl / l^2$ or $Dl = c\, Dn / n^2$. In terms of the observable quantity, n , the resulting linewidth can be written as:

$$I_R(n) = I_R(n_o) \quad \exp\left[\frac{-(n-n_o)^2}{s_R^2}\right] \tag{1.14}$$

where $I_R(n_o)$ is the observable maximum intensity and s_R^2 is the resulting variance of the Gaussian distribution (we suppose here that the dominant broadening process is Doppler or that the dominant process generates a Gaussian broadening). The standard deviation s_R is related to the resulting broadening Dn_R by:

$$s_R = (Dn_R) \,/\, 2\,(\ln 2)^{1/2} \tag{1.15}$$

1.2.2a Ion Temperature from a Pure Doppler Broadening

For the case where the broadening depends solely on the thermal motion (Doppler Broadening) we have (see internal report WVU-PL-039):

$$Dn_R = Dn_D = (8 \ln 2 \;\; kT_i\, n_o^2\, m_i^{-1}\, c^{-2})^{1/2} \tag{1.16}$$

where T_i , m_i are the temperature and mass of the ion (or neutral), respectively. In terms of the resulting variance we have:

$$s_R^2 = s_D^2 = 2 \;\; kT_i \;\; n_o^2 \;\; m_i^{-1} \;\; c^{-2} = a_D \;\; T_i \tag{1.17}$$

where a_D ($a_D = 2\, k\, n_o^2\, m_i^{-1}\, c^{-2}$) is the Doppler fitting parameter, which is the only different parameter for each transition. Replacing a_D in equation (1.14) we obtain:

$$I_R(n) = I_R(n_o) \quad \exp\left[\frac{-(n-n_o)^2}{a_D\, T_i}\right] \tag{1.18}$$

Thus, the lineshape is expressed in terms of the species temperature. In terms of n and n_o in GHz, and T_i in eV, the fitting parameters for the four transitions considered here are:

$$\begin{aligned} &a_D^{-1}\,(\text{Ar II, 611.49 nm}) = .077408 \;\; \text{eV (GHz)}^{-2} \\ &a_D^{-1}\,(\text{Ar II, 664.37 nm}) = .091375 \;\; \text{eV (GHz)}^{-2} \\ &a_D^{-1}\,(\text{Ar II, 668.43 nm}) = .092495 \;\; \text{eV (GHz)}^{-2} \\ &a_D^{-1}\,(\text{He I, 587.57 nm}) = .007161 \;\; \text{eV (GHz)}^{-2} \end{aligned} \tag{1.19}$$

The pure Doppler broadening fit for the KaleidaGraph software is given by:

$$F(m_0, m_1, m_2, m_3) = m_1 * \exp\left(a_D^{-1} * (m_0 - m_2)^{\wedge 2} / m_3\right) ; m_1 = Amp; m_2 = n_o ; m_3 = T_i \quad (1.20)$$

Where m_0 is the independent variable (frequency in GHz) and the m_i (i = 1, 2, 3) are the guesses for the fit. Thus, m_1 is the amplitude of the Gaussian (close to zero; ≈ 0.1), m_2 is the central frequency (where maximum amplitude is observed, near zero when the laser is perfectly centered) and m_3 is the ion temperature (usually between 0.1 and 0.7 eV). The code uses the guesses as starting point and calculates the best fit yielding T_i (see example in section 4.2)

1.2.2b Ion Temperature for a Large Doppler and Small Zeeman Broadening (1st Order Approximation)

For the case of a small Zeeman splitting and large Doppler broadening (the Zeeman contribution is small but not completely negligible) we have

$$\Delta\nu_R \approx \Delta\nu_D + \Delta\nu_Z \quad , \quad (1.21)$$

where $\Delta\nu_Z$ is the Zeeman broadening. The resulting variance σ_R becomes

$$\sigma_R = a_D^{1/2} T_i^{1/2} + \Delta\nu_Z / 2\,(\ln 2)^{1/2} \quad (1.22)$$

Defining g as the effective Zeeman broadening at 1 kGauss:

$$g = \Delta\nu_Z(\mathrm{B} = 1\ \mathrm{kGauss}) / 2\,(\ln 2)^{1/2} \quad (1.23)$$

Since Zeeman Broadening increases linearly with magnetic field strength, equation (1.22) can be written as:

$$\sigma_R = a_D^{1/2} T_i^{1/2} + g\,B \quad (1.24)$$

where B is the magnetic field strength. Replacing equation (1.24) in equation (1.14) we have:

$$I_R(\nu) = I_R(\nu_o) \exp\left[\frac{-(\nu - \nu_o)^2}{(a_D^{1/2} T_i^{1/2} + g\,B)^2}\right] \quad (1.25)$$

Thus, the resulting lineshape is a function of the ion temperature and the magnetic field strength. This expression is valid for both p and s components. Of course, for the s components, ν_o is no longer the central frequency and two temperature fits can be obtained from the fluorescence spectrum (see example in section 4.2). All other parameters can be calculated for each condition. By replacing B = 0 in equation (1.25), one finds equation (1.18) as expected. In terms of the fit for the KaleidaGraph software we have:

$$F(m_0, m_1, m_2, m_3) = m_1 * \exp\left((a^2 m_3 + b m_3^{1/2} + c^2)^{-1} * (m_0 - m_2)^2\right) \quad , \quad (1.26)$$

where m_i is as defined above: $m_1 = Amp$; $m_2 = n_o$; $m_3 = T_i$. and the a, b, c terms defined are given by:

$$a = a_D^{1/2}, \qquad b = 2\, a_D^{1/2}\, g\, B \quad \text{and,} \qquad c = g\, B \tag{1.27}$$

The dependence on T_i is now quadratic. a is the pure Doppler term, b represents a mix of Doppler-Zeeman terms, and c is a pure Zeeman term (see example in section 4.3). Again, if B = 0, expression (1.27) reduces to (1.20); fit for a simple Doppler broadening.

1.3 ION TEMPERATURE BY A DE-CONVOLUTION TECHNIQUE

For the helicon plasmas, the resulting fluorescence lineshape is a convolution of Doppler broadening and Zeeman splitting. Each component of the observed Zeeman splitting is broadened by thermal motion (Doppler broadening). Thus, the resulting lineshape can be best described as the envelope that encompasses all of the different Doppler broadened Zeeman components.

To perform the de-convolution, we must first introduce an expression that describes the resulting lineshape envelope. The resulting intensity function is a series of superimposed Gaussian distributions (of different intensities) each located at a different frequency shift with respect to the central frequency. The Zeeman splitting determines positions and locations of each Gaussian distributions. The resulting intensity function can be written as:

$$I_R(n) = \sum_{i=1}^{n} I_i(n_o - \Delta n_i)\ \exp\left[\frac{-(n - \Delta n_i - n_o)^2}{s_D^{\,2}}\right] \tag{1.28}$$

where Dn_i and $I_i\ (n_o - Dn_i)$ are the spacing relative to the central frequency n_o and the relative intensities of the different n Zeeman components, respectively. Each Zeeman component is broadened by thermal motion. The resulting variance s_D^2 is simply:

$$s_D^{\,2} = \frac{2kn_o^{\,2}}{c^2 m_i}(T_i)\ , \tag{1.29}$$

which is the variance of a pure Doppler broadening (see section 1.2.2a). The Dn_i 's can be written in terms of the central frequency and the magnetic field strength B:

$$Dn_i = \pm\ e_i\, n_o\, B \qquad , \tag{1.30}$$

where the e_i are shift coefficients for each Zeeman component with respect to the central frequency. The + and – signs indicate that the Zeeman components are located on both sides of the central frequency (symmetric for the p component, a bit more complex for the s components; see example in sections 4.2 and 4.3). For B = 0, expression (1.28) reduces to equation (1.18), the pure Doppler Broadening lineshape function. In terms of the fit for the KaleidaGraph software we have for p component broadening:

$$F(m_0, m_1, m_2, m_3) = m_1 \sum_{i=1}^{n/2} A_i \left[\exp(-a_D^{-1}(m_0 - e_i n_o B - m_2)^2 / m_3) + \exp(-a_D^{-1}(m_0 + e_i n_o B - m_2)^2 / m_3)\right] \quad (1.31)$$

where A_i is the statistical weight (or amplitude) of the Zeeman component (one of equal amplitude on each side of the central wavelength). Because of the symmetric nature of the Zeeman splitting, this summation only contains $n/2$ terms. For the s components, there is no symmetry (the amplitudes are different on each side of the central frequency) and the fit can be written as:

$$F(m_0, m_1, m_2, m_3) = m_1 \sum_{i=1}^{n} A_i \left[\exp(-a_D^{-1}(m_0 \pm e_i n_o B - m_2)^2 / m_3)\right] , \quad (1.32)$$

where the summation is over n terms with the ± sign related to the position of the Zeeman component with respect to the central frequency of the fluorescence signal. It is often convenient to separate the 2 clusters to evaluate the ion temperature. By using solely the $+ Dn_i$ ($Dn_i = e_i n_o B$) one finds the right cluster while the $-Dn_i$ yields the left cluster (see sections 4.2 and 4.3). In all cases, the m_i parameters have the same meaning as in the pure Doppler broadening and the Zeeman-Doppler broadening (1st order approximation). Examples of the different types of de-convolution are given in section 4.3.

2.0 ZEEMAN SPLITTING FOR THE Ar II 611 nm TRANSITION

For a 1 kGauss magnetic field and for our LIF pump line (level $3d^2G_{9/2}$ to level $4p^2F^0_{7/2}$) the Zeeman splitting is, according to equation (1.5a);

$$D\lambda = 1.74 \times 10^{-2} \text{ Å } (g_1M_1 - g_2M_2) \qquad (2.1)$$

Landé fractional factors for both levels of our LIF system are calculated in this section. A description of the possible values of the magnetic orbital number M_j for both levels is given in Fig. 2.1. For the metastable level, M_j varies between -9/2 and 9/2 (M_j changes by unit values only), while for the excited level; M_j varies between -7/2 and 7/2. An example of both *p* and *s* transitions is also shown in Fig. 2.1. According to the Ar II Grotrian diagram [Bashkin], the possible values for the quantum number *L*, *S* and *J* for the 2 levels [Herzberg] are:

L = 4 for $3d^2G_{9/2}$ (G-term; doublet),
L = 3 for $4p^2F^0_{7/2}$ (F-term; doublet),
S = 1/2 (doublet) for both levels,
J = 9/2 for $3d^2G_{9/2}$,
J = 7/2 for $4p^2F^0_{7/2}$
M_j = 9/2, 7/2, 5/2, 3/2 …….-9/2 for $3d^2G_{9/2}$
M_j = 7/2, 5/2, 3/2, 1/2 ……...-7/2 for $4p^2F^0_{7/2}$
λ = 611.49 nm (611.66 nm, vacuum)

Using equation (1.2) we obtain the Landé factors for the 2 levels:

$$g(3d^2G_{9/2}) = 10/9 \qquad \text{and} \qquad g(4p^2F^0_{7/2}) = 8/7$$

The Zeeman splitting is calculated using the Landé factors and is shown in tables 2.1 and 2.2. Due to the symmetry of the Zeeman pattern, each Zeeman component needs only to be considered on one side of the central wavelength. For the *p* transitions, the magnetic orbital quantum number for each level is the same ($M_j = M_1 = M_2$); the calculated values for a 1 kGauss magnetic field are shown in table 2.1. For the *s* transitions, the magnetic orbital quantum number for each levels is different ($M_1 - M_2 = \pm 1$); the calculated values (B = 1 kGauss) are shown in table 2.2.

The statistical weights for all the *p*-components are calculated using equation (1.8) and shown in table 2.1. In a similar fashion, the statistical weights for all the *s*-components are calculated and shown in table 2.2.

2.1 Ar II 611 nm ZEEMAN BROADENING (1ST ORDER APPROXIMATION)

The *p* components are symmetrically distributed around the central unshifted line. The different components with their relative statistical weight are shown in Fig. 2a. For a 1 kGauss magnetic field, the Zeeman broadening associated with the *p* components is:

$$D\lambda_{Zp} = 2.6 \times 10^{-3} \text{ Å}$$

Fig. 2.1 Zeeman splitting for the Ar II 611 nm transition

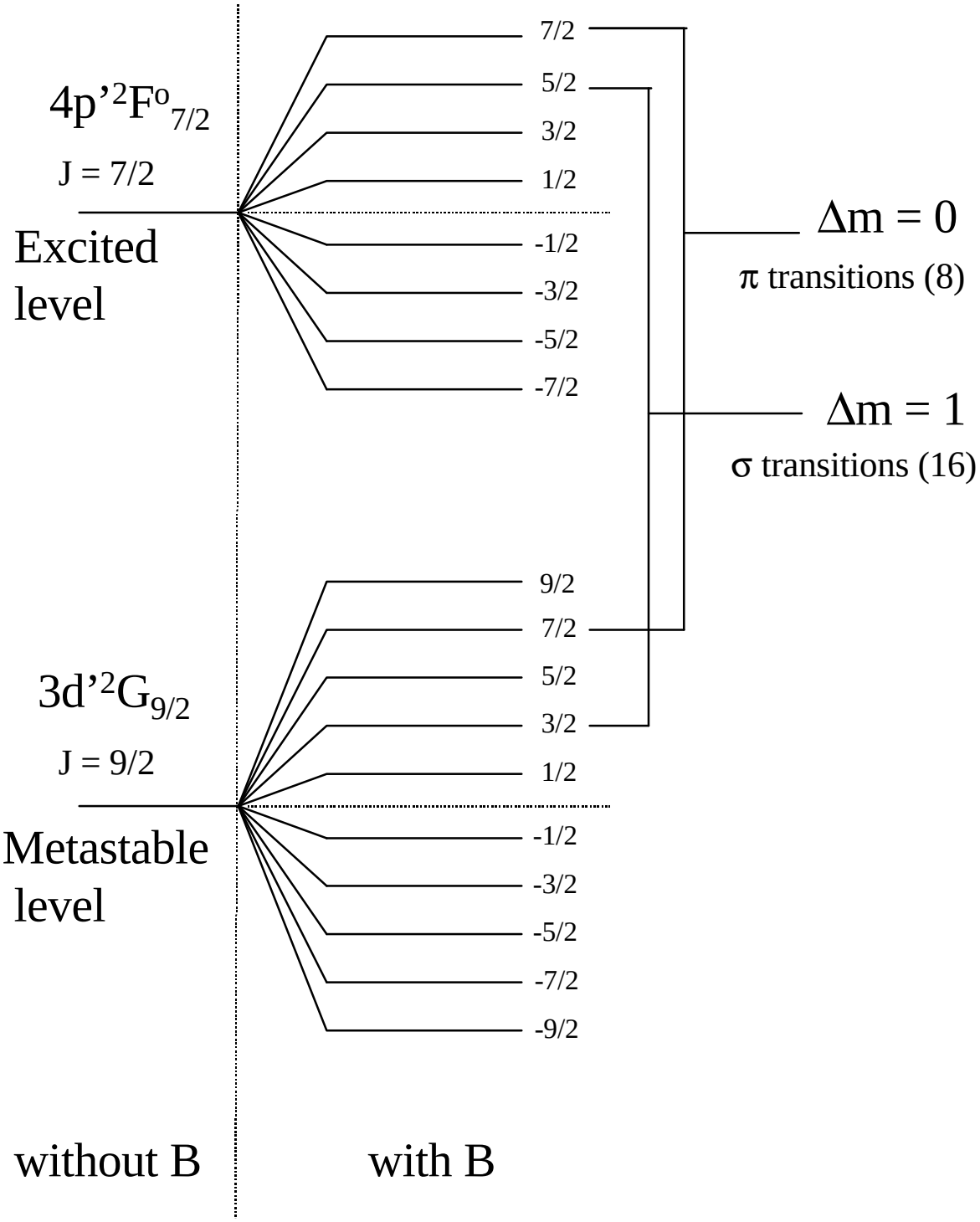

Fig. 2.2 Ar II 611Å nm Zeeman Components

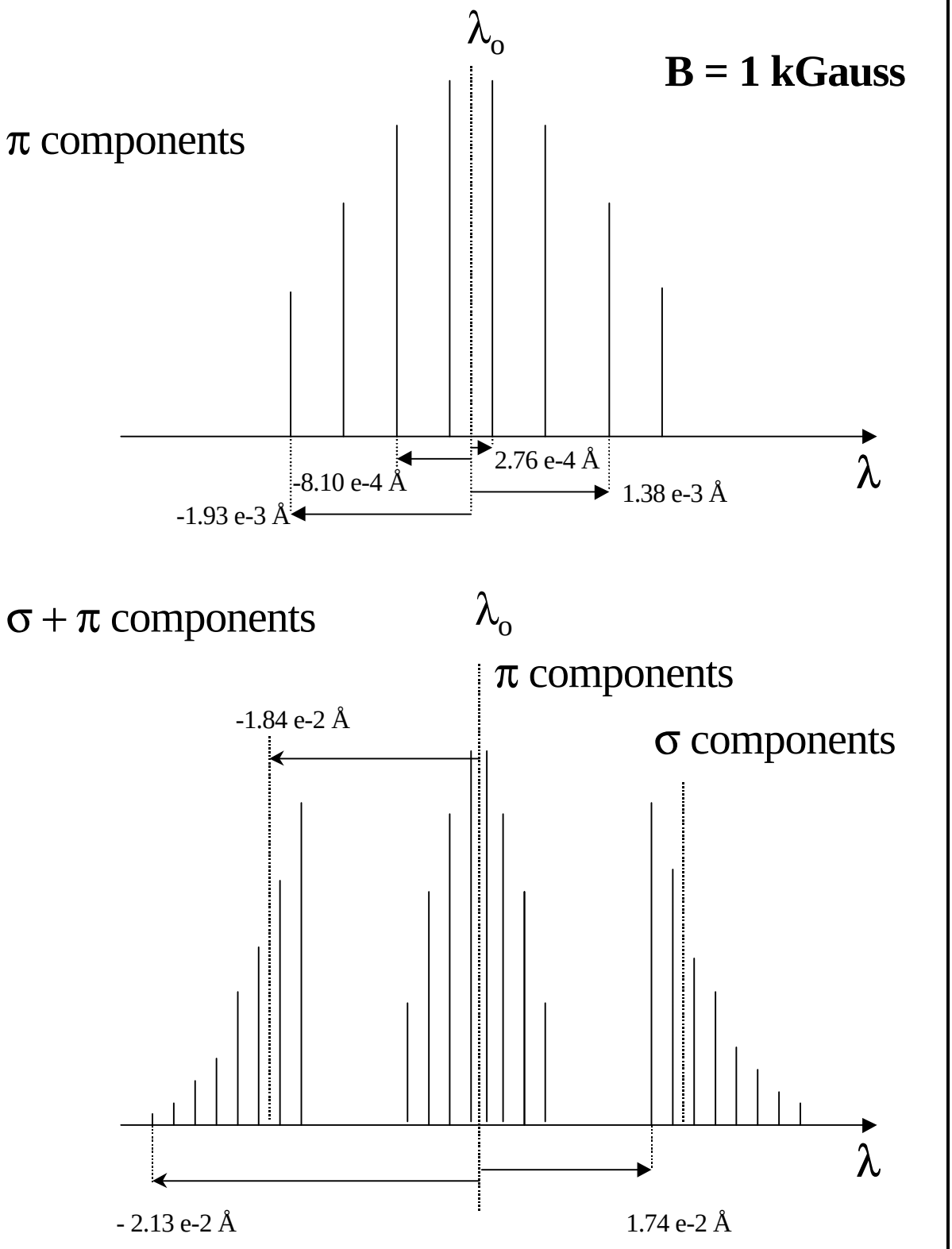

Two clusters of lines are symmetrically shifted on each side of the central line. The distribution pattern is shown in Fig 2b. Each cluster is asymmetric with the most intense lines closest to the central wavelength. First, we calculate the average wavelength shift by:

$$m_l = \sum_i l_i / n = 1.84 \times 10^{-2} \text{ Å} \qquad (2.2)$$

which means that the average shift of the s components is $\pm$ 1.84 x 10^{-2} Å with respect to the unshifted central wavelength. We now use equations (1.10) and (1.11) to calculate the FWHM. For a 1 kGauss magnetic field, the Zeeman Broadening associated with the s components is:

$$\Delta l_{Zs} = 2.2 \times 10^{-3} \text{ Å}$$

Because of the asymmetry of the cluster, we can suppose that the real Δl_s is probably a bit larger:

$$\Delta l_{Zs} \gg \Delta l_{Zp} \approx 2.6 \times 10^{-3} \text{ Å}$$

Table 1.1

Zeeman splitting for the p transitions ($M = M_1 = M_2$)

M	$(g_1 - g_2)M$	Δl (Å)	w
7/2	7/63	1.93 x 10^{-3}	0.0333
5/2	5/63	1.38 x 10^{-3}	0.0583
3/2	3/63	8.10 x 10^{-4}	0.0750
1/2	1/63	2.76 x 10^{-4}	0.0833

+ 4 symmetric components

Table 1.2

Zeeman splitting for the s transitions ($M_1 \neq M_2$):

M_1	M_2	$g_1M_1 - g_2M_2$	Δl (Å)	w
9/2	7/2	63/63	1.74 x 10^{-2}	0.0750
7/2	5/2	65/63	1.79 x 10^{-2}	0.0583
5/2	3/2	67/63	1.85 x 10^{-2}	0.0438
3/2	1/2	69/63	1.91 x 10^{-2}	0.0313
1/2	-1/2	71/63	1.96 x 10^{-2}	0.0208
-1/2	-3/2	73/63	2.02 x 10^{-2}	0.0125
-3/2	-5/2	75/63	2.07 x 10^{-2}	0.0063
-5/2	-7/2	77/63	2.13 x 10^{-2}	0.0021

+ 8 symmetric components

Thus, for the 611 nm transition, the effective Zeeman broadening (either the π or σ polarization) for a 1 kGauss magnetic field is according to equation (1.23):

$$\gamma \approx 1.249 \times 10^{8} \text{ Hz} \bullet (\text{kGauss})^{-1} \text{ or } 0.1249 \text{ GHz} \bullet (\text{kGauss})^{-1}.$$

with α_D^{-1} given in (1.19), we have

$$\alpha_D^{1/2} \approx 3.594 \times 10^{9} \text{ Hz} \bullet (\text{eV})^{-1/2} \text{ or } 3.594 \text{ GHz} \bullet (\text{eV})^{-1/2})$$

and equation (1.24), becomes (both terms are in GHz),

$$s_R = a_D^{1/2} T_i^{1/2} + g B = 3.594 T_i^{1/2} + 0.1249 B \qquad \text{(in GHz)} \qquad (2.3)$$

Replacing this value in equation (1.25), the ion temperature (in eV) can be determined from the measured lineshape. A detailed description of the exact de-convolution technique is given in section 4.2 for the Ar II 668 nm transition. A similar approach must be used to exactly fit this specific transition.

3.0 ZEEMAN SPLITTING FOR THE Ar II 664 nm TRANSITION

For a 1 kGauss magnetic field, the Zeeman splitting for the Ar II 664 nm pump line (level $3d^4F_{9/2}$ to level $4p^4D^0_{7/2}$) is according to equation (1.5a);

$$\Delta\lambda = 2.05 \times 10^{-2} \text{ Å } (g_1M_1 - g_2M_2) \qquad (3.1)$$

Landé fractional factors for both levels of this LIF scheme are calculated in this section. A description of the possible values of the magnetic orbital number M_j for both levels is given in Fig. 3.1. For the metastable level, M_j varies between -9/2 and 9/2 (M_j changes by unit values only), while for the excited level, M_j varies between -7/2 and 7/2. An example of both *p* and *s* transitions is also shown in Fig. 1. According to the Ar II Grotrian diagram [Bashkin], the possible values for the quantum number *L, S, J* for the 2 levels [Herzberg] are:

L = 3 for $3d^4F_{9/2}$ (F-term; quartet),
L = 2 for $4p^4D^0_{7/2}$ (D-term; quartet),
S = 3/2 (quartet) for both levels,
J = 9/2 for $3d^4F_{9/2}$,
J = 7/2 for $4p^4D^0_{7/2}$
M_j = 9/2, 7/2, 5/2, 3/2 …….-9/2 for $3d^4F_{9/2}$
M_j = 7/2, 5/2, 3/2, 1/2 …….-7/2 for $4p^4D^0_{7/2}$
λ = 664.37 nm (664.55 nm, vacuum)

Using equation (1.2) we obtain the Landé factors for the 2 levels:

$g(3d^4F_{9/2}) = 28/21$ (or 4/3) and $g(4p^4D^0_{7/2}) = 30/21$ (or 10/7)

The Zeeman splitting is calculated using the expression above and shown in tables 3.1 and 3.2. Due to the symmetry of the Zeeman pattern, each Zeeman component needs only to be considered on one side of the central wavelength. For the *p* transitions, the magnetic orbital quantum number for each levels is the same ($M_j = M_1 = M_2$); the calculated values for a 1 kGauss magnetic field are shown in table 3.1. For the *s* transitions, the magnetic orbital quantum number for each levels is different ($M_1 - M_2 = \pm 1$); the calculated values (B = 1 kGauss) are shown in table 3.2.

The statistical weights for all the *p*-components are calculated using equations (1.7 to 1.9) and shown in table 3.1. In a similar fashion, the statistical weights for all the *s*-components are calculated and shown in table 3.2.

3.1 Ar II 664 nm ZEEMAN BROADENING (1ST ORDER APPROXIMATION)

The *p* components are symmetrically distributed around the central unshifted line. The different components with their relative statistical weight are shown in Fig. 3a. In the case of a 1 kGauss magnetic field, the Zeeman broadening associated with the *p* components is

$$\Delta\lambda_{Zp} = 9.0 \times 10^{-3} \text{ Å}$$

Fig. 3.1 Zeeman splitting for the Ar II 664 nm Transition

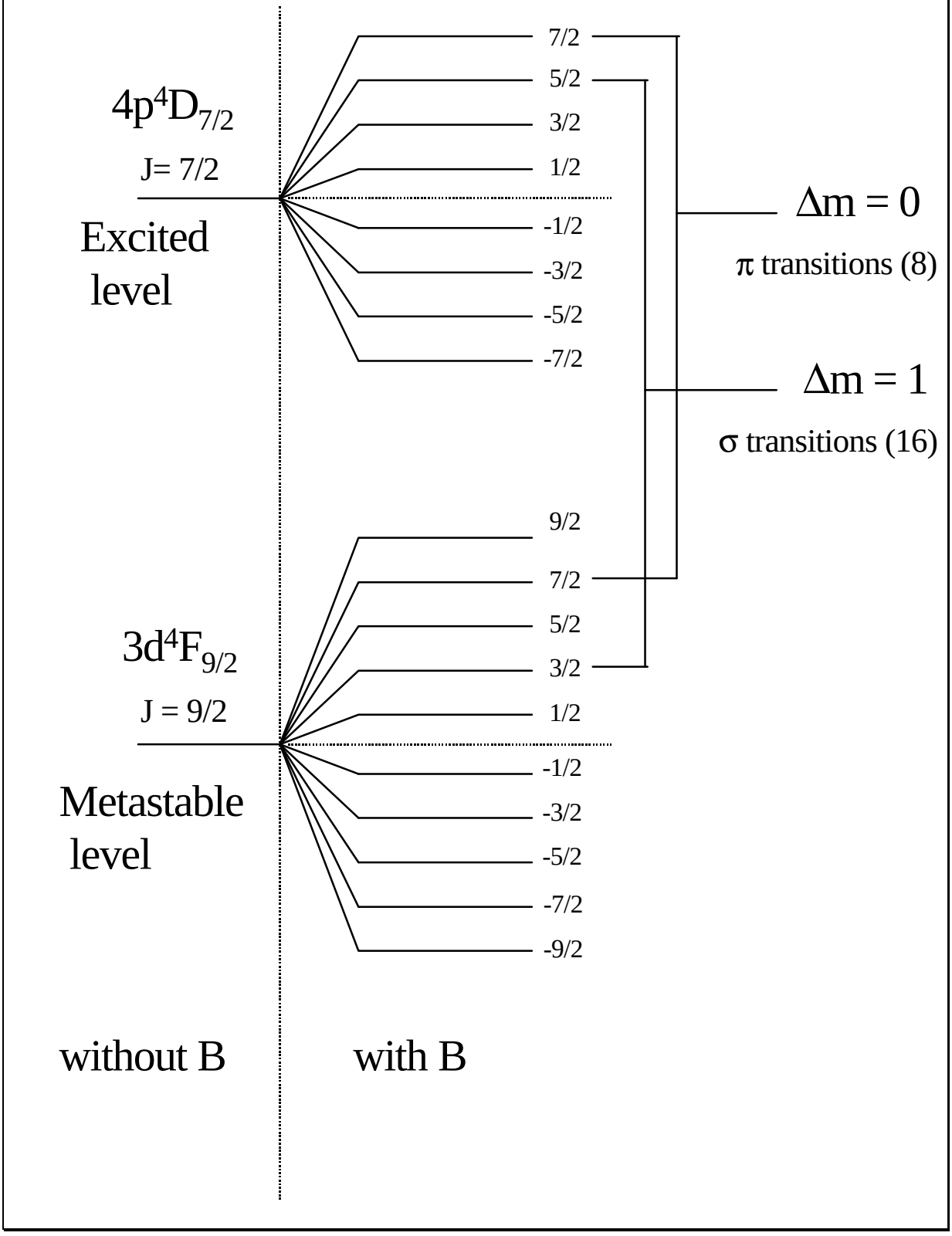

Fig. 3.2 Ar II 664 nm Zeeman Components

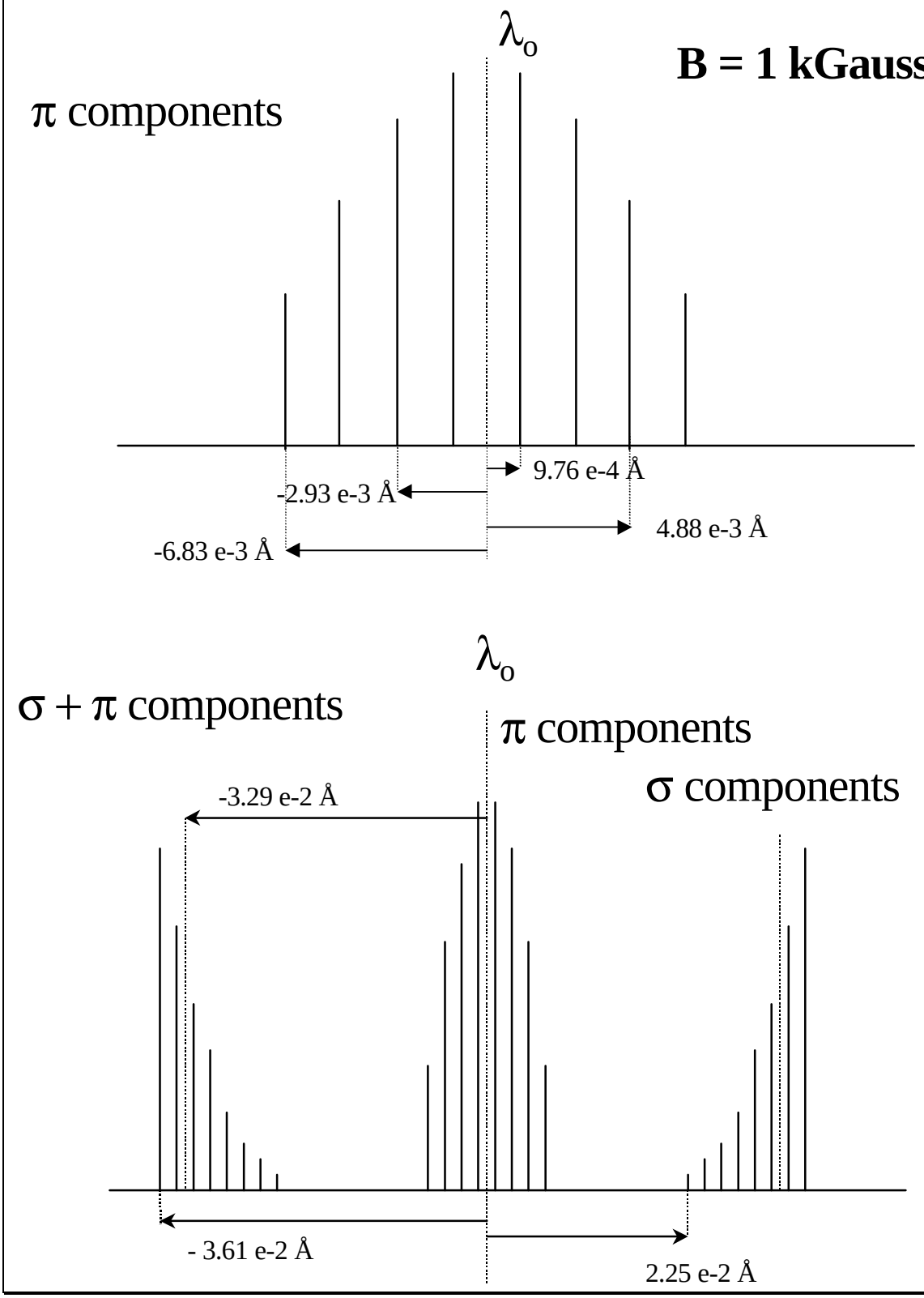

The two clusters of line are symmetrically shifted to each side of the central line. The distribution pattern is shown in Fig 3b. Each cluster is asymmetric with the most intense lines farthest from the central wavelength. First, we calculate the average wavelength by:

$$m_l = \sum_i l_i / n = 3.29 \times 10^{-2} \text{ Å} \qquad (3.2)$$

which yields on average shift of the s components of $\pm$ 3.29 x 10^{-2} Å with respect to the unshifted central wavelength. We now use equations (1.10) and (1.11) to calculate the FWHM. For a 1 kGauss magnetic field, the Zeeman Broadening associated with the s components is:

$$\Delta\lambda_{Zs} = 7.8 \times 10^{-3} \text{ Å}$$

Because of the asymmetry of the cluster, we can suppose that the real $\Delta\lambda_s$ is probably a bit larger:

$$\Delta\lambda_{Zs} \approx 8.5 \times 10^{-3} \text{ Å}$$

Note that the Zeeman broadenings for both the π and σ transitions are more than 3 times larger than the Zeeman broadening for the 611 nm line.

Table 3.1

Zeeman splitting for the p transitions ($M = M_1 = M_2$)

M	$(g_1 - g_2)M$	$\Delta\lambda$ (Å)	w
7/2	7/21	6.83 x 10^{-3}	0.0333
5/2	5/21	4.88 x 10^{-3}	0.0583
3/2	3/21	2.93 x 10^{-3}	0.0750
1/2	1/21	9.76 x 10^{-4}	0.0833

+ 4 symmetrical components

Table 3.2

Zeeman splitting for the s transitions ($M_1 \neq M_2$):

M_1	M_2	$g_1M_1 - g_2M_2$	$\Delta\lambda$ (Å)	w
9/2	7/2	37/21	3.61 x 10^{-2}	0.0750
7/2	5/2	35/21	3.41 x 10^{-2}	0.0583
5/2	3/2	33/21	3.22 x 10^{-2}	0.0438
3/2	1/2	31/21	3.03 x 10^{-2}	0.0313
1/2	-1/2	29/31	2.83 x 10^{-2}	0.0208
-1/2	-3/2	27/31	2.64 x 10^{-2}	0.0125
-3/2	-5/2	25/31	2.44 x 10^{-2}	0.0063
-5/2	-7/2	23/31	2.25 x 10^{-2}	0.0021

+ 8 symmetrical components

Thus, for this 664 nm transition, the effective Zeeman broadening for a 1 kGauss magnetic field is:

$$\gamma \approx 0.3263 \text{ GHz} \bullet (\text{kGauss})^{-1}$$

α_D^{-1} as defined in equation (1.19) is:

$$\alpha_D^{1/2} \approx 3.308 \text{ GHz} \bullet (\text{eV})^{-1/2})$$

and equation (1.24) can now be written as;

$$s_R = a_D^{1/2} T_i^{1/2} + g B = 3.308 T_i^{1/2} + 0.3263 B \qquad \text{(in GHz)} \qquad (3.3)$$

This expression for s_R can be used in equation (1.26) to extract the ion temperature (in eV) from the measured lineshape. The exact de-convolution technique described in sections 4.2 and 4.3 can also be used to obtain the ion temperature.

4.0 ZEEMAN SPLITTING FOR THE Ar II 668 nm TRANSITION

For a 1 kGauss magnetic field, the Zeeman splitting for the Ar II 668 nm pump transition (level $3d^4F_{7/2}$ to level $4p^4D_{5/2}$) is according to equation (1.5a);

$$\Delta\lambda = 2.08 \times 10^{-2} \text{ Å } (g_1M_1 - g_2M_2) \qquad (4.1)$$

Landé fractional factors for both levels of this LIF scheme are now calculated. A description of the possible values of the magnetic orbital number M_j for both levels is given in Fig. 4.1. For the metastable level, M_j varies between -7/2 and 7/2 (M_j changes by unit values only), while for the excited level, M_j varies between -5/2 and 5/2. An example of both *p* and *s* transitions is also shown in Fig. 4.1. According to the Ar II Grotrian diagram [Bashkin], the possible values for the quantum number *L, S, J* for the 2 levels [Herzberg] are:

L = 3 for $3d^4F_{7/2}$ (F-term; quartet),
L = 2 for $4p^4D_{5/2}$ (D-term; quartet),
S = 3/2 (quartet) for both levels,
J = 7/2 for $3d^4F_{7/2}$,
J = 5/2 for $4p^4D_{5/2}$
M_j = 7/2, 5/2, 3/2 …….-7/2 for $3d^4F_{7/2}$
M_j = 5/2, 3/2,1/2 ……..-5/2 for $4p^4D_{5/2}$
λ = 668.43 nm (668.61 nm, vacuum)

Using equation (1.2) we obtain the Landé factors for the 2 levels:

$$g(3d^4F_{7/2}) = 130/105 \quad \text{and} \quad g(4p^4D_{5/2}) = 144/105$$

The Zeeman splitting is calculated using the expression above and shown in tables 4.1 and 4.2. Due to the symmetry of the Zeeman pattern, each Zeeman component needs only to be considered on one side of the central wavelength. For the *p* transitions, the magnetic orbital quantum number for each levels is the same ($M_j = M_1 = M_2$); the calculated values for a 1 kGauss magnetic field are shown in table 4.1. For the *s* transitions, the magnetic orbital quantum number for each levels is different ($M_1 - M_2 = \pm 1$); the calculated values (B = 1 kGauss) are shown in table 4.2.

The statistical weights for all the *p*-components are calculated using equations (1.7 to 1.9) and shown in table 4.1. In a similar fashion the statistical weights for all the *s*-components are calculated and shown in table 4.2.

4.1 Ar II 668 nm ZEEMAN BROADENING (1ST ORDER APPROXIMATION)

The *p* components are symmetrically distributed around the central unshifted line. The different components with their relative statistical weight are shown in Fig. 4a. In the case of a 1 kGauss magnetic field, the Zeeman broadening associated with the *p* components is:

$$\Delta\lambda_{Zp} = 9.8 \times 10^{-3} \text{ Å}$$

Fig. 4.1 Zeeman splitting for the Ar II 668 nm Transition

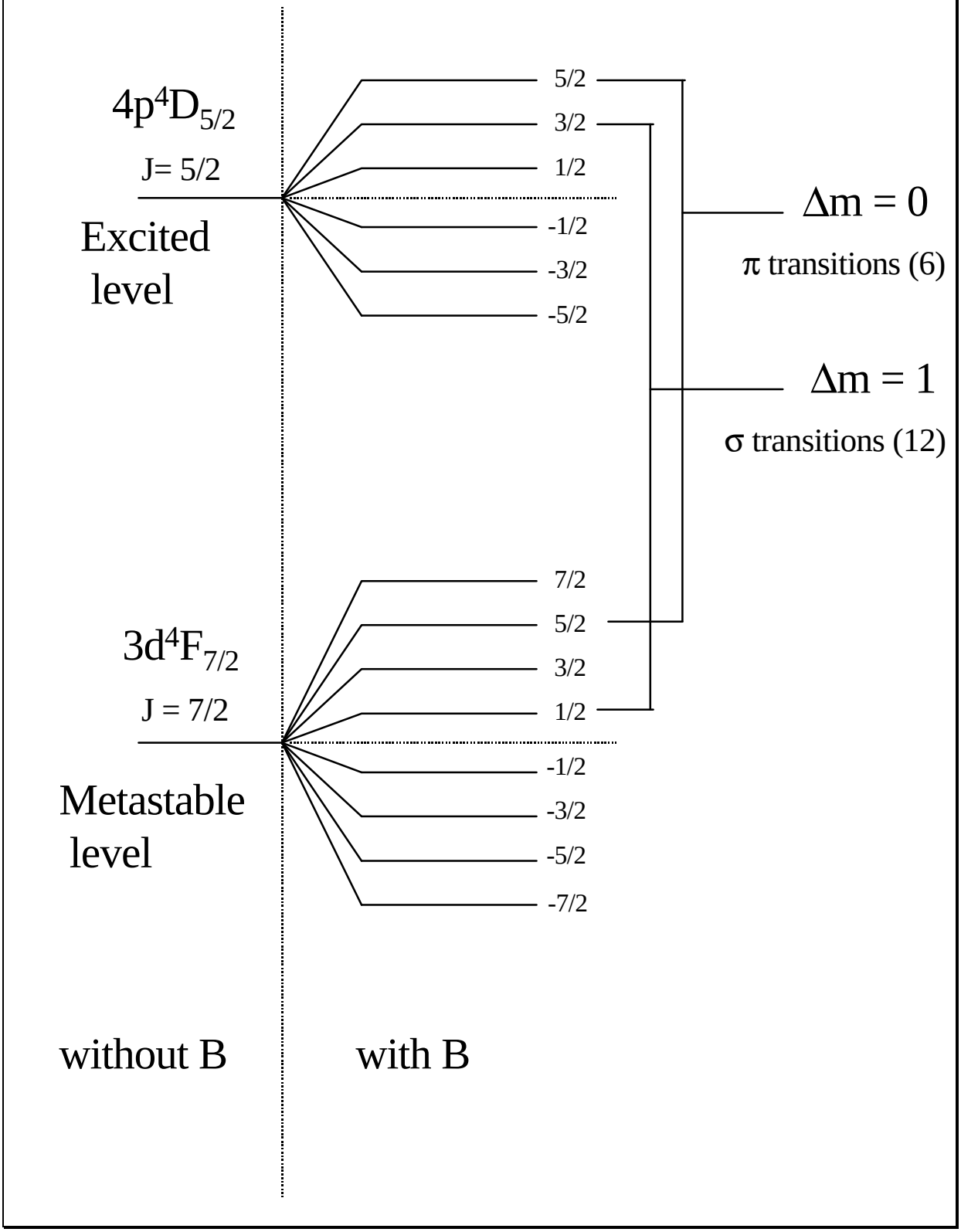

Fig. 4.2 Ar II 668 nm Zeeman Components

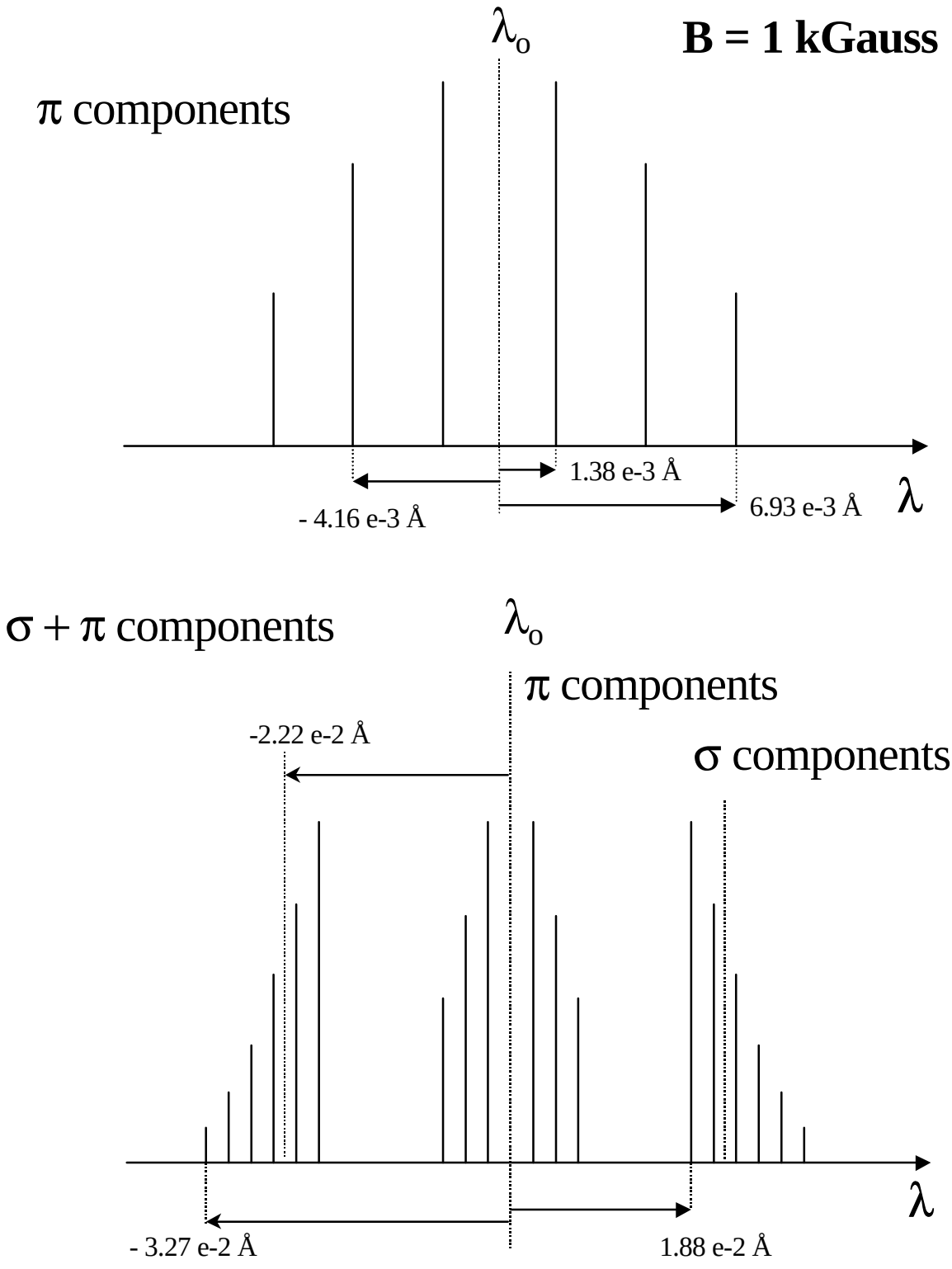

Two clusters of line are symmetrically shifted on each side of the central line. The distribution pattern is shown in Fig 4b. Each cluster is asymmetric with the most intense lines closest to the central wavelength. First, we calculate the average wavelength given by:

$$m_l = \sum_i l_i / n = 2.22 \times 10^{-2} \text{ Å} \qquad (4.2)$$

which means that the average shift of the *s* components is ± 2.22 x 10^{-2} Å with respect to the unshifted central wavelength. We now use equations (1.10) and (1.11) to calculate the FWHM. For a 1 kGauss magnetic field, the Zeeman Broadening associated with the *s* components is:

$$\Delta l_{Zs} \approx 8.5 \times 10^{-3} \text{ Å}$$

Because of the asymmetry of the cluster, we can suppose that the real Δl_s is probably a bit larger:

$$\Delta l_{Zs} \approx 9.0 \times 10^{-3} \text{ Å}$$

Again, these broadenings are much larger than in the case of the 611 nm transition

Table 4.1

Zeeman splitting for the *p* transitions *($M = M_1 = M_2$)*

M	$(g_1 - g_2)M$	Δl (Å)	w
5/2	5/15	6.93 x 10^{-3}	0.0536
3/2	3/15	4.16 x 10^{-3}	0.0892
1/2	1/15	1.38 x 10^{-3}	0.1071

+ 3 symmetrical components

Table 4.2

Zeeman splitting for the *s* transitions ($M_1 \neq M_2$):

M_1	M_2	$g_1M_1 - g_2M_2$	Δl (Å)	w
7/2	5/2	95/105	1.88 x 10^{-2}	0.09375
5/2	3/2	109/105	2.15 x 10^{-2}	0.06696
3/2	1/2	123/105	2.43 x 10^{-2}	0.04464
1/2	-1/2	137/105	2.71 x 10^{-2}	0.02679
-1/2	-3/2	151/105	2.99 x 10^{-2}	0.01339
-3/2	-5/2	165/105	3.27 x 10^{-2}	0.00446

+ 6 symmetrical components

Thus, for this 668 nm transition, the effective Zeeman broadenings for a 1 kGauss magnetic field are according to equation (1.23):

$$\gamma(\pi) \approx 0.3627 \text{ GHz} \bullet (\text{kGauss})^{-1}$$

$$\gamma(\sigma) \approx 0.3331 \text{ GHz} \bullet (\text{kGauss})^{-1}$$

where the effective Zeeman Broadening for the σ-components is slightly smaller than the corresponding value for the π-component (see above). α_D^{-1} given in (1.19), thus we have:

$$\alpha_D^{1/2} \approx 3.288 \text{ GHz} \bullet (\text{eV})^{-1/2})$$

We now use equation (1.24);

$$s_R(\pi) = a_D^{1/2} T_i^{1/2} + g B = 3.288 T_i^{1/2} + 0.3627 B \quad \text{in (GHz)}$$

$$s_R(\sigma) = a_D^{1/2} T_i^{1/2} + g B = 3.288 T_i^{1/2} + 0.3331 B \quad \text{in (GHz)}$$

The ion temperature can be determined from the measured lineshapes (π and σ transitions) by using these s_R expressions in equation (1.26).

4.2 Ar II 668 nm EXACT DE-CONVOLUTION TECHNIQUE

To exactly de-convolute the 668-nm lineshape we first require the exponential Doppler factor (equation (1.29)), which can be written for this transition as:

$$s_R^2 = (\alpha_D \ T_i)^{-1} \approx .092495 / T_i \qquad (4.3)$$

Equation (1.28) can then be written as

$$I_R(n) = \sum_{i=1}^{n} I_i(n_o - \Delta n_i) \ \exp\left[\frac{-.092495 \ (n - \Delta n_i - n_o)^2}{T_i}\right] \qquad (4.4)$$

The shifts of the different Zeeman components can be calculated from equation 1.30. Let us first consider the de-convolution for the π-component. From table 4.1, the frequency shifts of the 6 π-components are (B = 1 kGauss):

$\Delta\nu_1 = \pm 0.0926$ GHz	$w_1 = .1071$
$\Delta\nu_2 = \pm 0.279$ GHz	$w_2 = .0892$
$\Delta\nu_3 = \pm 0.465$ GHz	$w_3 = .0536$

where the w_i are the statistical weights associated with each Zeeman component. The 6 π-components represents only 50 % of the total line intensity (the other 50 % is divided equally in the 2 remaining σ clusters; see equation 1.8). Since we are considering a signal composed solely

of π-components (chosen polarization) we must multiply each statistical weight by 2. Replacing the numerical values in equation (4.4), the lineshape function becomes:

$$I_R(n) = .2142 \exp\left[\frac{-.092495(n \pm .0926\,B - n_o)^2}{T_i}\right] + \tag{4.5}$$

$$.1784 \exp\left[\frac{-.092495\,(n \pm 0.279B - n_o)^2}{T_i}\right] + .1072 \exp\left[\frac{-.092495\,(n \pm 0.465B - n_o)^2}{T_i}\right]$$

where the ± signs are associated with the symmetric π-components (6 terms) and B is the magnetic field intensity in kGauss. The parameterization of this formula for the Kaleidagraph program is given in the next section.

For the σ-components, there are 12 terms, 6 per each cluster. Here, there is no symmetry around the average frequency shift of each cluster. Let us consider the right cluster (positive sign on the frequency displacement). From table 4.1, the frequency shifts of the 6 σ right components are:

$\Delta\nu_1 =$ + 1.26 GHz	$w_1 = .0938$
$\Delta\nu_2 =$ + 1.44 GHz	$w_2 = .0670$
$\Delta\nu_3 =$ + 1.63 GHz	$w_3 = .0446$
$\Delta\nu_4 =$ + 1.82 GHz	$w_4 = .0268$
$\Delta\nu_5 =$ + 2.01 GHz	$w_5 = .0134$
$\Delta\nu_6 =$ + 2.19 GHz	$w_6 = .00446$

Each σ cluster corresponds to 25% of the total intensity (see equation 1.8). Thus, in the analysis of the measured lineshape, the statistical weight of each component must be multiplied by 4. The resulting lineshape function for the right σ line cluster is given by:

$$I_R(n) = .375 \exp\left[\frac{-.092495\,(n + 1.26\,B - n_o)^2}{T_i}\right] + .268 \exp\left[\frac{-.092495\,(n + 1.44\,B - n_o)^2}{T_i}\right] +$$

$$.179 \exp\left[\frac{-.092495\,(n + 1.63\,B - n_o)^2}{T_i}\right] + .107 \exp\left[\frac{-.092495\,(n + 1.82\,B - n_o)^2}{T_i}\right] +$$

$$.0536 \exp\left[\frac{-.092495\,(n + 2.01\,B - n_o)^2}{T_i}\right] + .0178 \exp\left[\frac{-.092495\,(n + 2.19\,B - n_o)^2}{T_i}\right] \tag{4.6}$$

The parameterization of this formula for the Kaleidagraph program is given in the next section. The left σ cluster linehape function is obtained by changing the sign for Dn_i ($Dn_i = - e_i\, n_o B$).

4.3 T_i EVALUATION FROM THE RESULTING LINESHAPE (EXAMPLES)

4.3.1 π-components

4.3.1a Pure Doppler Fit

Let us consider the de-convolution technique for the π-components. The plasma conditions for the ion temperature measurements are (File 64, 8/24/01):

Plasma Source	=	MNX Device
RF Power	=	250 Watts
Magnetic Field Intensity	=	1.8 kGauss
Discharge Pressure	=	6.6 mTorr (Argon)
Wavelength	=	668.43 nm (0.02 nm sweep)

The LIF fluorescence signal is fitted with the pure Doppler Broadening expression (equation 1.18) with $\alpha_D^{-1} = 0.092495$ eV $(GHz)^{-2}$. The KaleidaGraph fit used was,

m1*exp(-.092495*(M0-m2)^ 2/m3 ; m1=.1; m2=.5; m3=.4

The fit to the data shown in Fig. 4.3 yields an ion temperature of 0.29 eV. The other fit parameters are given in Fig. 4.3.

Fig. 4.3

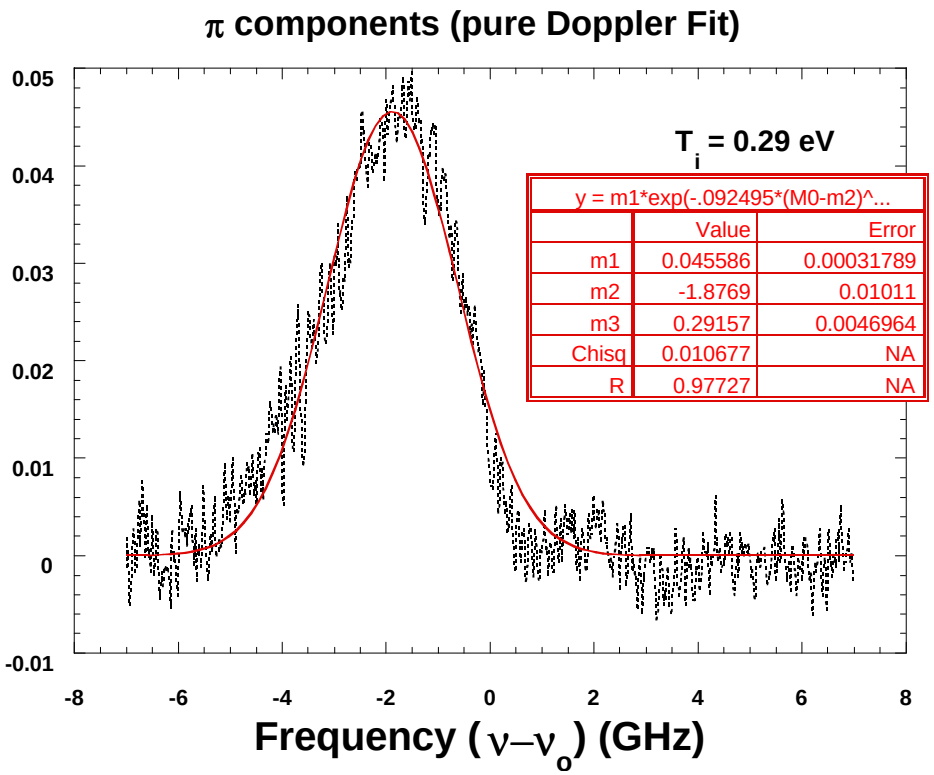

4.3.1b Doppler- Zeeman Fit (1st Order Approximation)

We now recalculate the ion temperature using the Doppler-Zeeman 1st order approximation. For the 668 nm transition, the variance according to section 4.1 is:

$$s_R^2 = (a_D^{1/2} T_i^{1/2} + g B)^2 \approx (10.81\, T_i + 2.385\, B\, T_i^{1/2} + .1316\, B^2)$$

Since the *B* field intensity is 1.8 kGauss, the Kaleidagraph fit was written as:

m1* exp(-(0.1316*(1.8)^ 2 + 2.385* (1.8) * m3^ 1/2 + 10.81*m3)^-1*(M0-m2)^ 2)
; m1=.05; m2=-1.5; m3=.25

and the 1st order Doppler-Zeeman fit is shown in Fig. 4.4.

Fig. 4.4

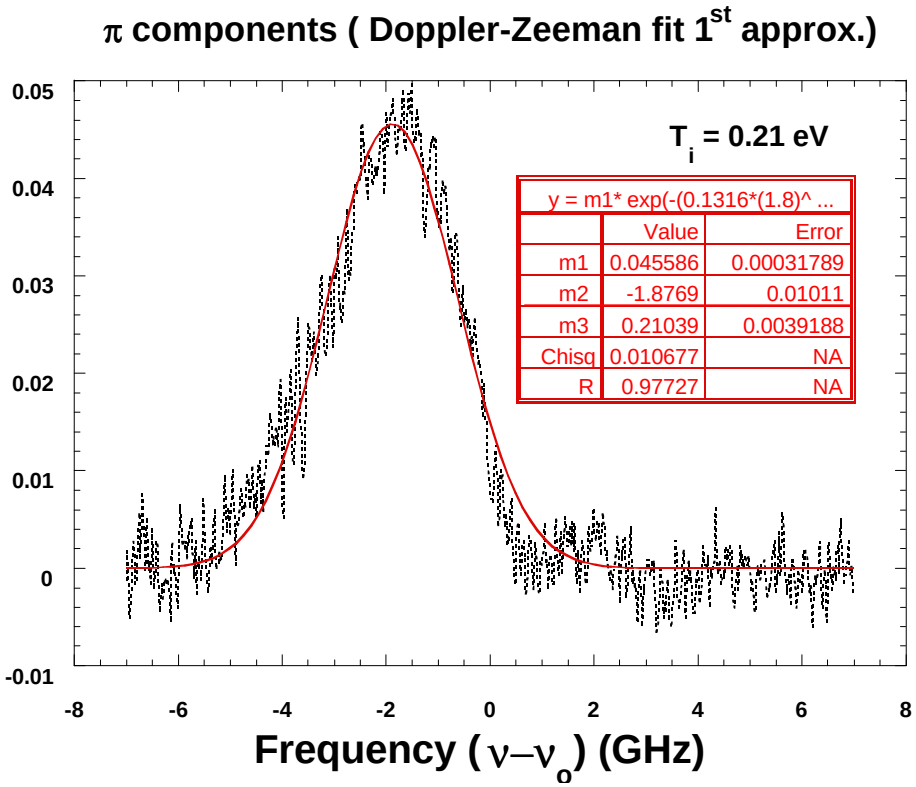

The fitted ion temperature of 0.21 eV is lower than for the fit assuming a pure Doppler broadening. This approach usually over corrects the Zeeman contribution to the resulting lineshape since the calculation only approximates Zeeman Broadening (see section 1.2.2a). Thus, we expect that the de-convolution formula should yield an ion temperature between 0.21 and 0.29 eV.

4.3.1c De-Convolution Fit

We now use the de-convolution formula as defined in section 4.2. Using equation (4.5) with a 1.8 Kgauss magnetic field, the Kaleidagraph fit was written as:

m1*(.214*((exp(-.0925*(M0-.0926*(1.8)-m2)^2/m3)+(exp(-0925*(M0+.0926*(1.8)-m2)^2/m3))
+.178*((exp(-.0925*(M0-.279*(1.8)-m2)^2/m3)+(exp(-.0925*(M0+.279*(1.8)-m2)^2/m3))
+.107*((exp(-.0925*(M0-.465*(1.8)- m2)^2/m3)+(exp(-.0925*(M0+.465*(1.8)-m2)^2/m3)))

;m1=.05;m2=-1.5;m3=.25

Unfortunately this form is too long for the Kaleidagraph program. By multiplying the different terms in the exponential factors, the expression simplifies to:

m1*(.214*(exp(-.0925*(M0-.167-m2)^ 2/m3)+ exp(-.0925*(M0+.167-m2)^ 2/m3))
+.178*(exp(-.0925*(M0-.502-m2)^ 2/m3)+ exp(-.0925*(M0+.502-m2)^ 2/m3))
+.107*(exp(-.0925*(M0-.837- m2)^ 2/m3)+exp(-.0925*(M0+.837-m2)^ 2/m3)))

;m1=.05;m2=-1.5;m3=.25,

and the de-convolution fit is shown in Fig. 4.5.

Fig. 4.5

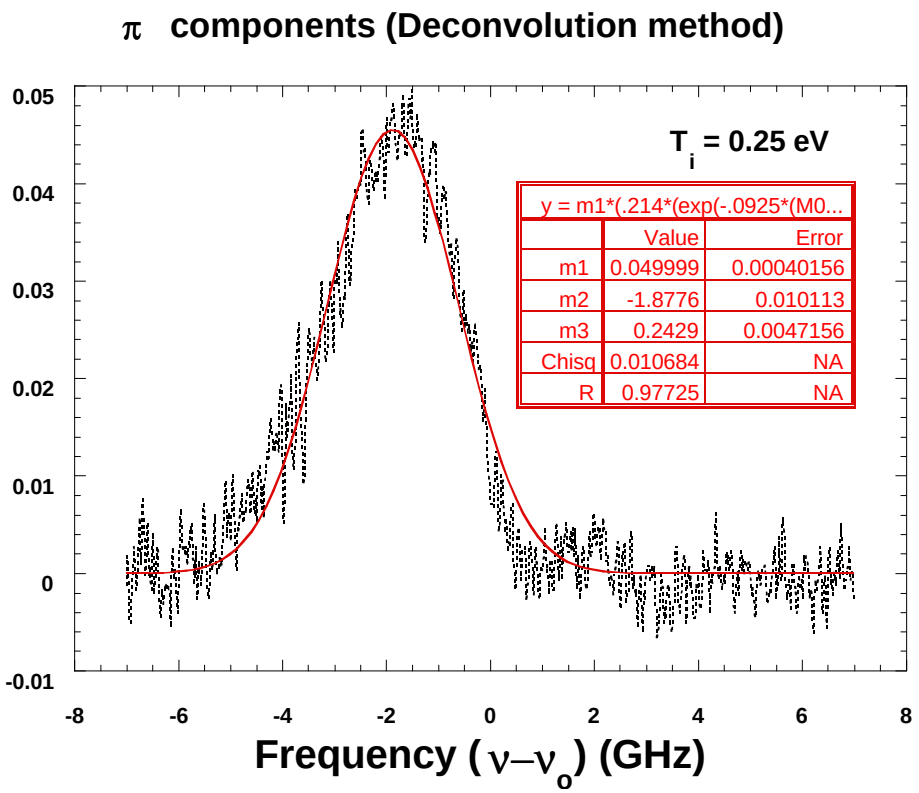

The de-convolution fit yields an ion temperature of 0.25 eV. This temperature is within the range defined by the ion temperature calculated using the pure Doppler fit and the Doppler-Zeeman 1st approximation fit.

4.3.2 σ-components

4.3.2a Pure Doppler Fit

Let us consider the de-convolution technique for the σ-components. The plasma conditions for the ion temperature measurements are (File 54, 8/21/01):

Plasma Source	=	MNX Device
RF Power	=	490 Watts
Magnetic Field Intensity	=	1.9 kGauss
Discharge Pressure	=	10.0 mTorr (Argon)
Wavelength	=	668.43 nm (0.02 nm sweep)

The LIF fluorescence signal is fitted with the pure Doppler broadened expression (equation 1.18) with $\alpha_D^{-1} = 0.092495$ eV $(GHz)^{-2}$. The KaleidaGraph fit of the first peak was:

m1*exp(-.092495*(M0-m2)^ 2/m3) ; m1=.1; m2=- 4.5; m3=.4

The pure Doppler fit for the first σ-cluster is shown in Fig. 4.6.

Fig. 4.6

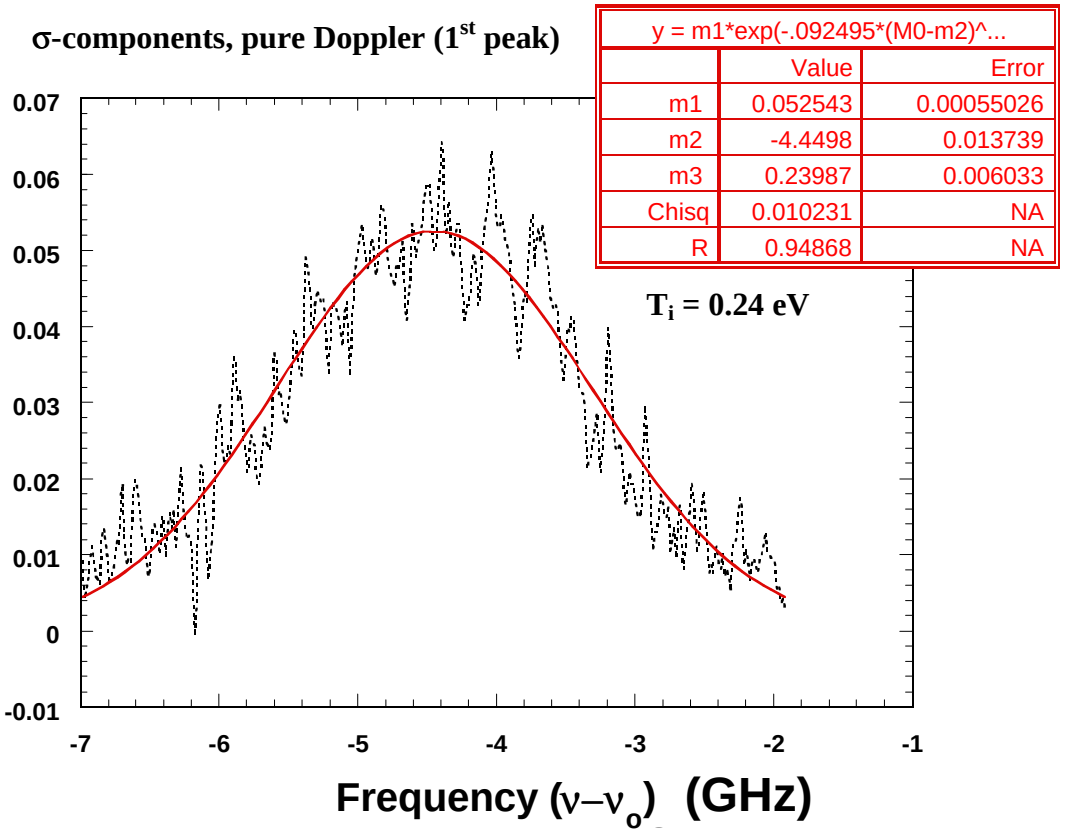

The pure Doppler fit for the first cluster of σ-lines yields an ion temperature of 0.24 eV.

The fit used for the second cluster of σ-lines is simply:

m1*exp(-.092495*(M0-m2)^ 2/m3) ; m1=.1; m2=4.5; m3=.4

where the m2 parameter is adjusted to a positive value (4.5). The pure Doppler fit for the second σ-cluster is shown in Fig. 4.7.

Fig. 4.7

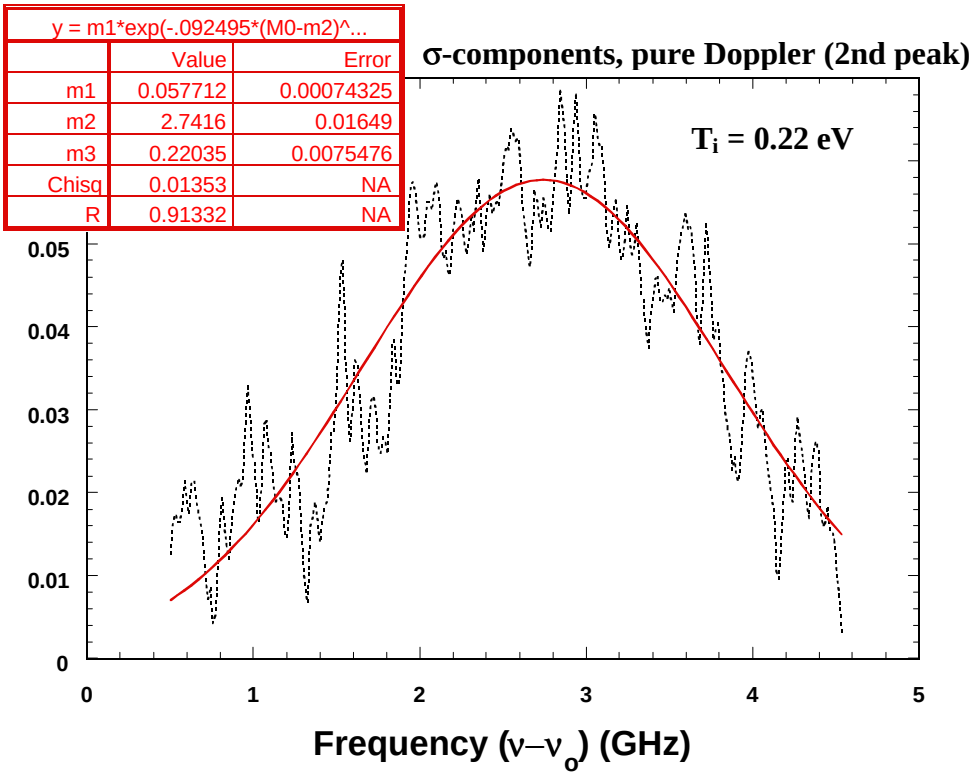

The pure Doppler fit yields an ion temperature of 0.22 eV (comparable to the previous value). Given the low quality of the S/N ratio, the 0.02 eV difference is remarkably small.

4.3.2b Doppler- Zeeman Fit (1st Order Approximation)

We now use the Doppler-Zeeman 1st order approximation to evaluate the ion temperature of the σ-lines. For the first σ-cluster and for a magnetic field of 1.9 kGauss, the fit used was:

m1* exp(-(0.1110*(1.9)^ 2 + 2.190* (1.9) * m3^ 1/2 + 10.81*m3)^-1*(M0-m2)^ 2)

; m1=.05; m2=-4.5; m3=.25

The 1st order Doppler-Zeeman fit for the first σ-cluster is shown in Fig. 4.8.

Fig. 4.8

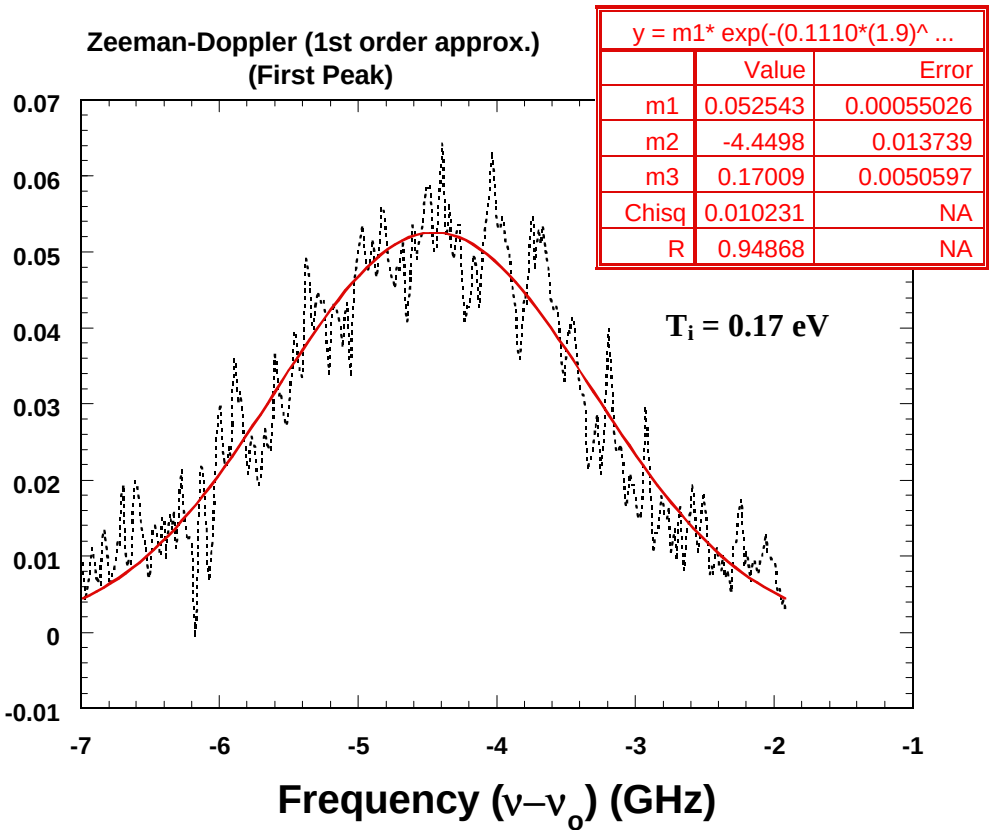

The 1st oder fit yields an ion temperature of about 0.17 eV. Again, this value is less than the one obtained with the pure Doppler fit, as expected.

For the second peak, only a minor adjustments in the code is needed (m2 = + 4.5);

m1* exp(-(0.1110*(1.9)^ 2 + 2.190* (1.9) * m3^ 1/2 + 10.81*m3)^-1*(M0-m2)^ 2)

; m1=.05; m2= 4.5; m3=.25.

The Doppler-Zeeman fit for the second σ-cluster is shown in Fig. 4.9

Fig. 4.9

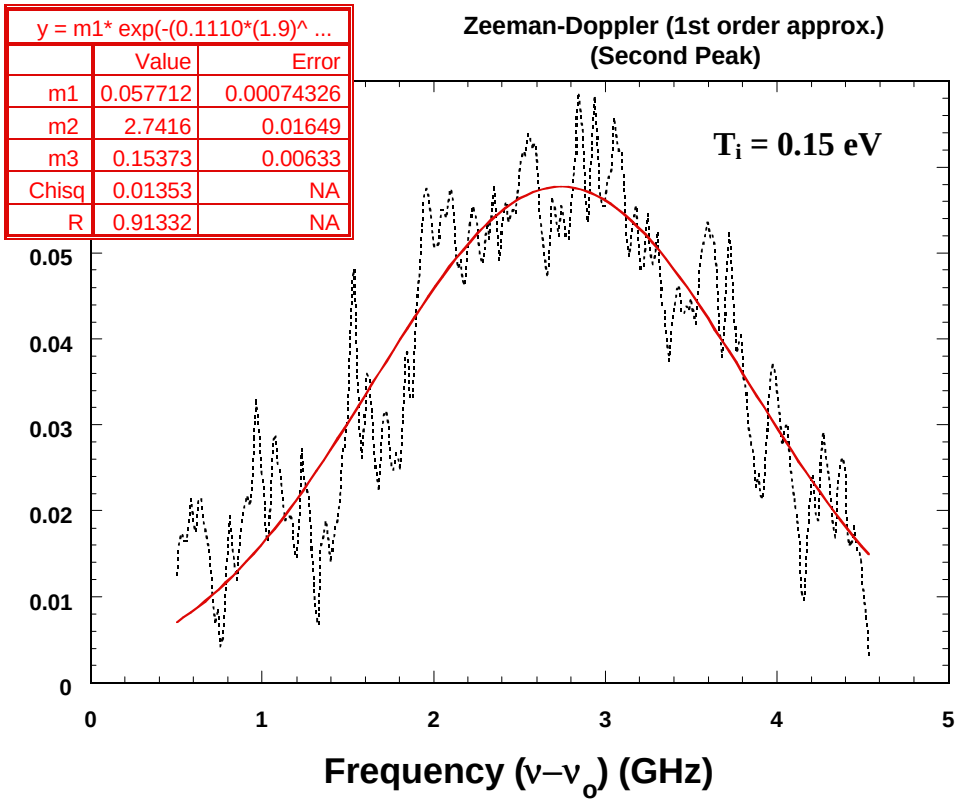

The 1st order fit yields an ion temperature of about 0.15 eV for the second σ-lines cluster. Note here, that the difference in temperature for the two peaks remains the same as the one obtained for the pure Doppler Fit. We expect that the ion temperature determined by the de-convolution fit should be between 0.17 and 0.24 eV for the first cluster and between 0.15 and 0.22 eV for the second σ-lines cluster.

4.3.2c De-Convolution Fit

For the first (or left) σ-lines cluster, the de-convolution fit is, according to equation (4.6), for a magnetic of 1.9 kGauss given by:

m1*(.375*exp(-.0925*(M0-2.39-m2)^2/m3) +.268*exp(-.0925*(M0-2.74-m2)^2/m3) +
.179*exp(-.0925*(M0-3.10-m2)^2/m3) + .107*exp(-.0925*(M0-3.46-m2)^2/m3) +
.0536*exp(-.0925*(M0-3.82-m2)^ 2/m3) + .0178*exp(-.0925*(M0-4.16-m2)^ 2/m3))

; m1=.03; m2=-4.0; m3=.25

The fit of the first σ-lines cluster using the de-convolution expression is shown in Fig. 4.10

Fig. 4.10

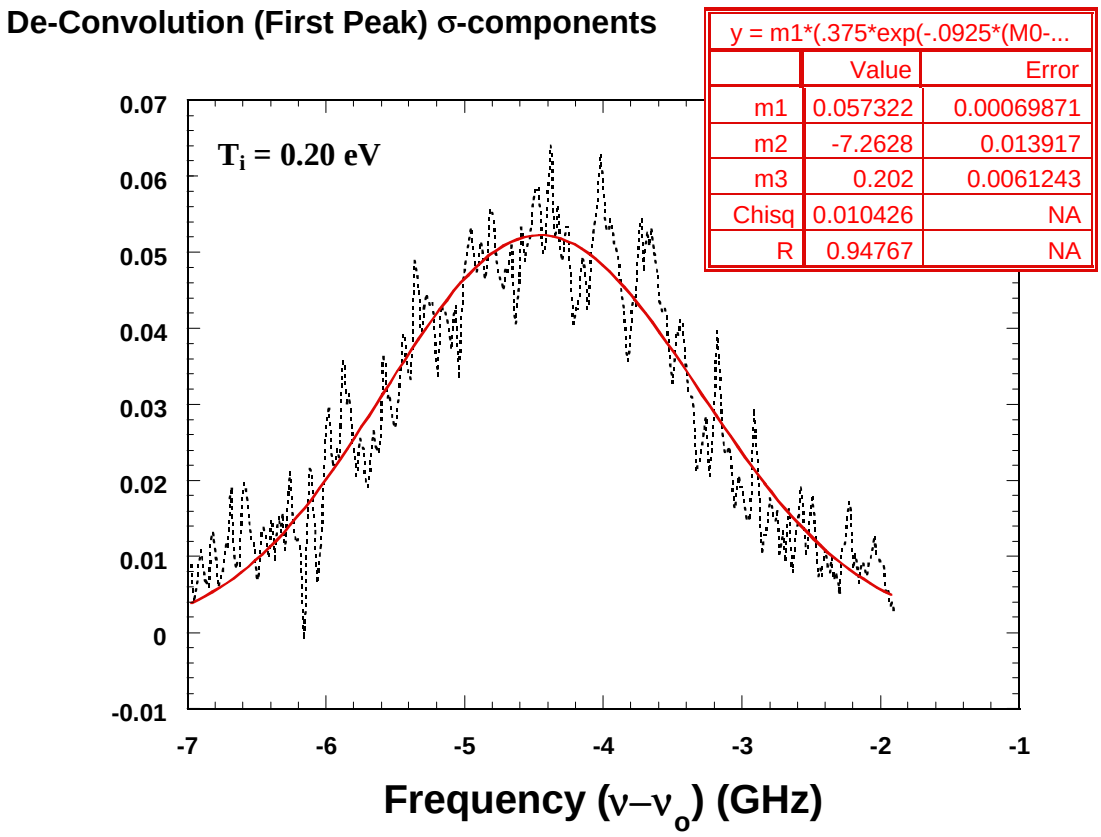

For the first cluster, the de-convolution fit yields an ion temperature of 0.20 eV (which is between 0.24 and 0.17 eV, as expected)

The second σ-lines cluster de-convolution expression is:

m1*(.375*exp(-.0925*(M0+2.39-m2)^ 2/m3) + .268*exp(-.0925*(M0+2.74-m2)^ 2/m3)+
.179*exp(-.0925*(M0+3.10-m2)^ 2/m3) + .107*exp(-.0925*(M0+3.46-m2)^ 2/m3)+
.0536*exp(-.0925*(M0+3.82-m2)^ 2/m3) + .0178*exp(-.0925*(M0+4.16-m2)^ 2/m3))

; m1=.03; m2=3.5; m3=.25 ,

where the second terms in the exponential factors are now positive. The fit to the second σ-lines cluster using the De-convolution expression is shown in Fig. 4.11.

Fig. 4.11

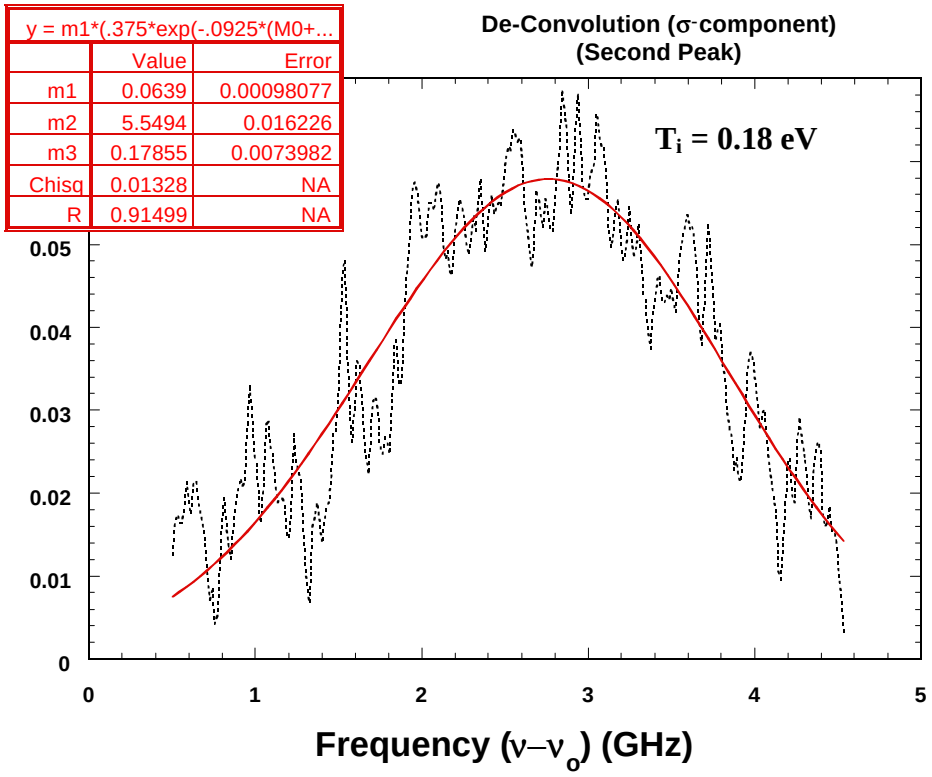

The de-convolution fit yields an ion temperature of 0.18 eV (which is between 0.22 and 0.15 eV, as expected).

5.0 ZEEMAN SPLITTING FOR THE He 587 nm TRANSITION

The Zeeman splitting of the 587 nm neutral helium line is again given by the expression (1.5a). For a 1 kGauss magnetic field and for the 587 nm LIF pump line (level 2^3P (J = 2) to level 3^3D (J = 3), Dl_z is:

$$Dl_z = 1.61 \times 10^{-2} \text{ Å } (g_1M_1 - g_2M_2) \qquad (5.1)$$

Landé fractional factors for both levels of this LIF system are calculated in this section. A description of the possible values of the magnetic orbital number M_j for both level is given in Fig. 5.1. For the upper level 3^3D, M_j varies between -3 and 3 (M_j changes by unit values only), while for the lower level 2^3P, M_j varies between -2 and 2. An example of both p and s transitions is also shown in Fig. 5.1. According to the He Grotrian diagram [Bashkin], the possible values for the quantum number L, S, J for the 2 levels [Herzberg] are:

L = 2 for 3^3D (D-term; triplet),
L = 1 for 2^3P (P-term; triplet),
S = 1 (triplet) for both levels,
J = 3 for 3^3D,
J = 2 for 2^3P
M_j = 3, 2, 1, 0, -1, -2, -3 for 3^3D
M_j = 2, 1, 0, -1, -2, for 2^3P
l = 587.57 nm (587.73 nm, vacuum)

The Landé factors are calculated by using equation 1.2 and we have for these 2 levels:

$$g(3^3\text{D}) = 4/3 \quad \text{and} \quad g(2^3\text{P}) = 3/2$$

The Zeeman splitting is calculated using equation (5.1) and shown in table 5.1 and 5.2. Due to the symmetry of the Zeeman pattern, Zeeman components need only to be calculated for one side of the central wavelength. For the p transitions, the magnetic orbital quantum number for each levels is the same ($M_j = M_1 = M_2$); the calculated values for a 1 kGauss magnetic field are shown in table 5.1. For the σ transitions, the magnetic orbital quantum number for each level is different ($M_1 - M_2 = \pm 1$); the calculated values (B = 1 kGauss) are shown in table 5.2.

The intensities of all Zeeman components for a $J \rightarrow J + 1$ transition are given by the expressions 1.7a and 1.7b. The statistical weights of all the p-components are calculated using the method described in section 1.1 and shown in table 5.1. In a similar fashion, the statistical weights for all the s-components are calculated and shown in table 5.2.

5.1 He I 587 nm ZEEMAN BROADENING (1ST ORDER APPROXIMATION)

The p components are symmetrically distributed around the central unshifted line. The different components with their relative statistical weight are shown in Fig. 5.2a.

Fig. 5.1 Zeeman Splitting for the He 587 nm transition

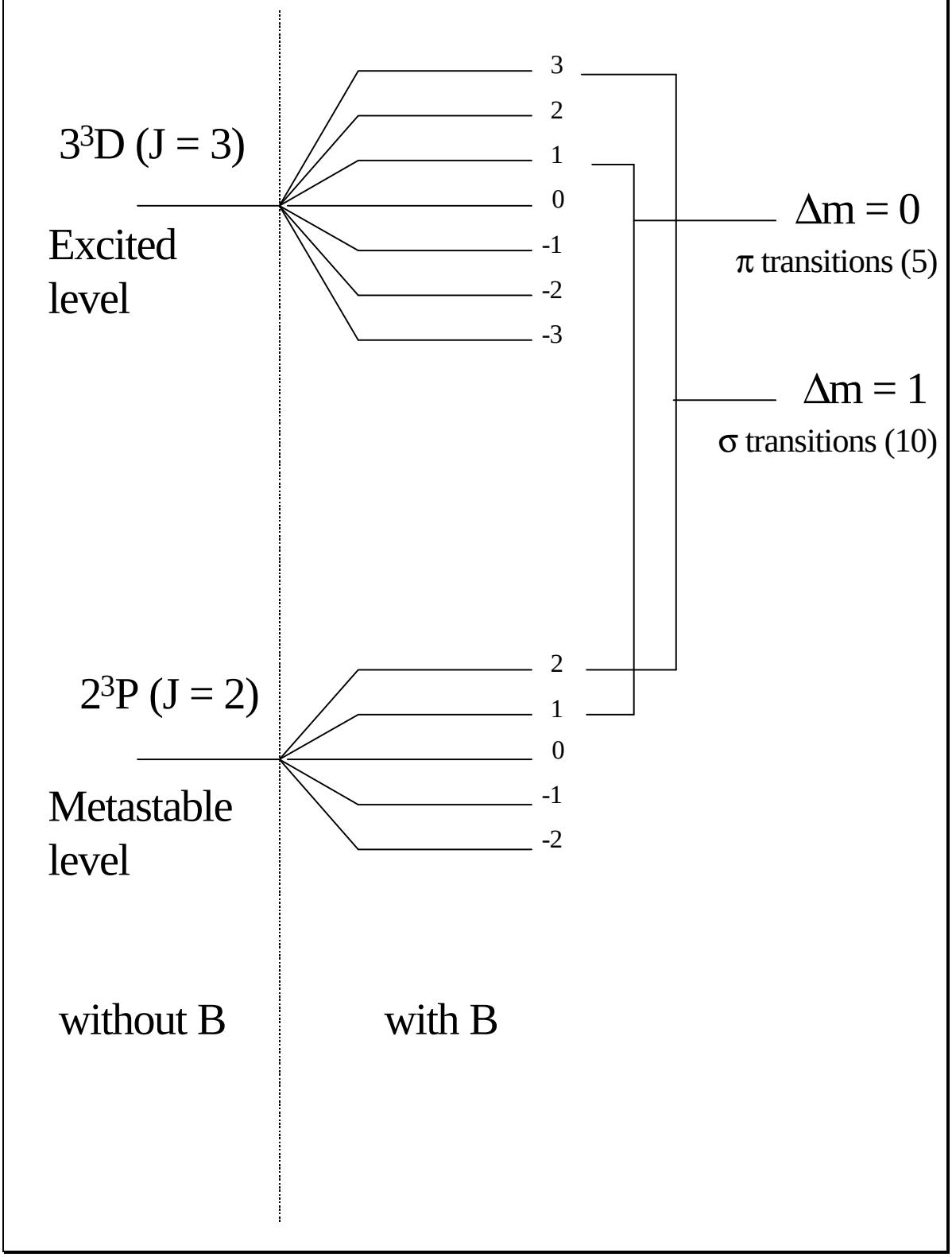

Fig. 5.2 He I 587 nm Zeeman Components

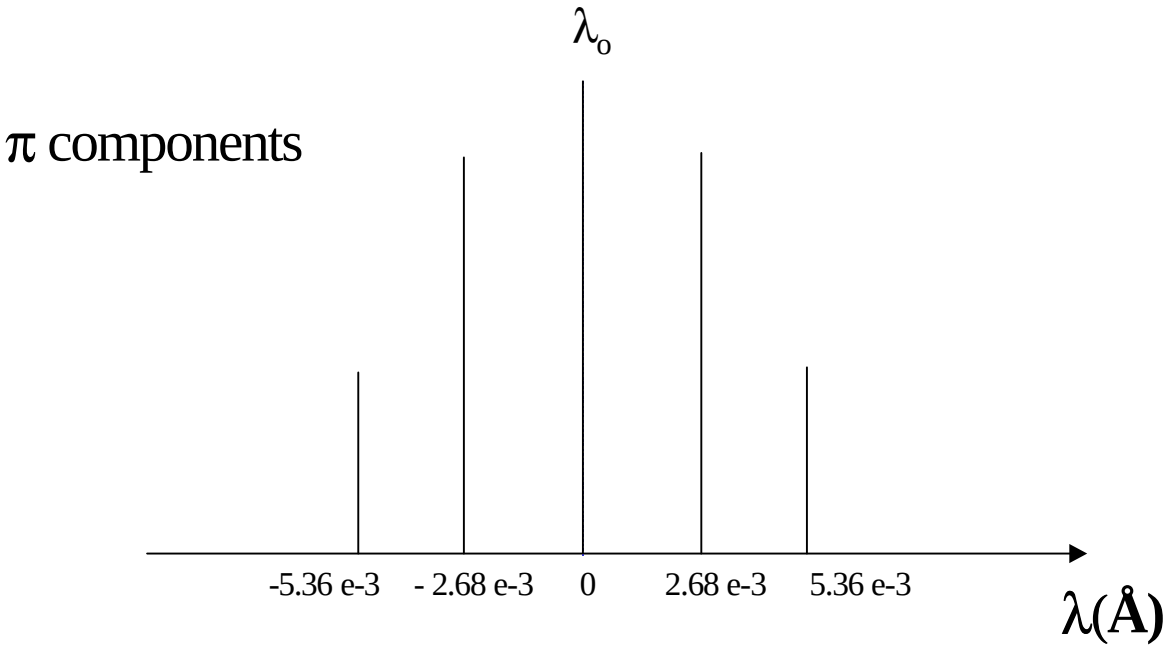

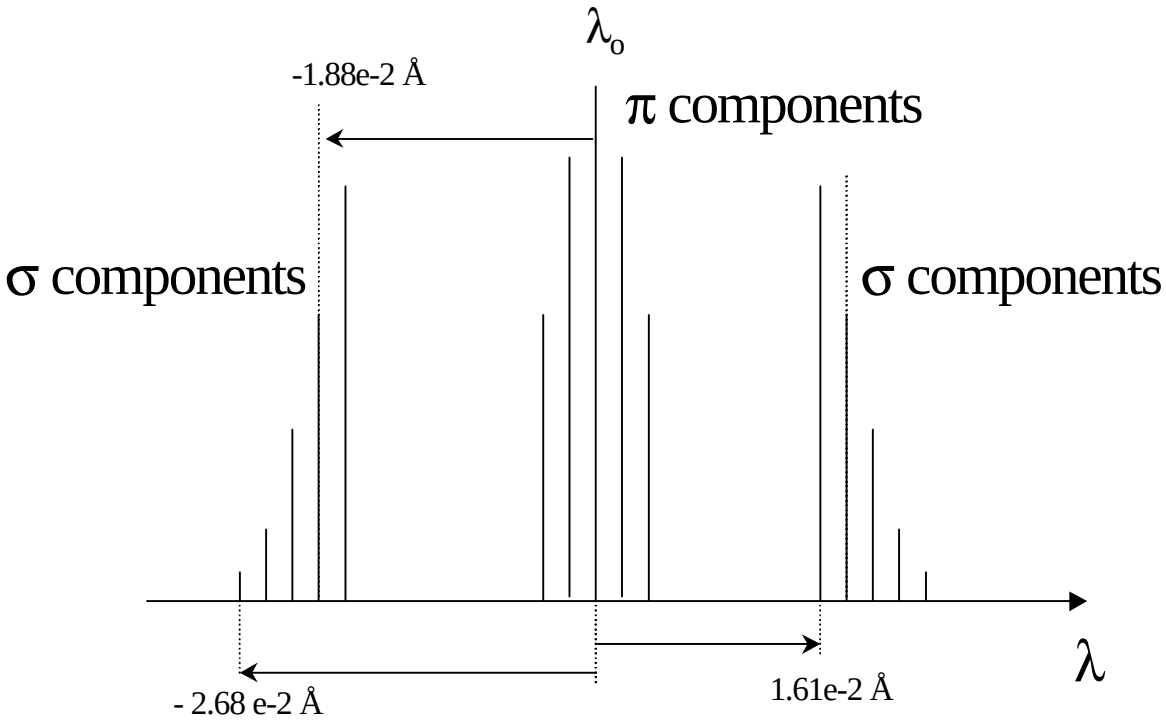

For a 1 kGauss magnetic field, the Zeeman broadening associated with the *p* components is:

$$\Delta\lambda_{Zp} = 7.98 \times 10^{-3} \text{ Å}$$

The two clusters of σ-lines are symmetrically shifted to each side of the central line. The distribution pattern is shown in Fig 5.2b. Each cluster is asymmetric with the most intense lines closest to the central wavelength. First, we calculate the average wavelength given by:

$$m_\lambda = \sum_i \lambda_i / n = 1.88 \times 10^{-2} \text{ Å}, \qquad (5.2)$$

which yields an average shift of the *s* components is ± 1.88 x 10^{-2} Å with respect to the unshifted central wavelength. We now use equations (1.7 to 1.9) to calculate the FWHM. For a 1 kGauss magnetic field, the Zeeman Broadening associated with the *s* components is:

$$\Delta\lambda_{Zs} = 6.95 \times 10^{-3} \text{ Å}.$$

Because of the asymmetry of the cluster, we can suppose that the real $\Delta\lambda_s$ is probably a bit larger,

$$\Delta\lambda_{Zs} \gg \Delta\lambda_{Zp} \approx 8.0 \times 10^{-3} \text{ Å},$$

Table 5.1
Zeeman splitting for the *p* transitions ($M = M_1 = M_2$)

M	$(g_1 - g_2)M$	½ $\Delta\lambda$ (Å) ½	I (K)	w
2	1/3	5.36 x 10^{-3}	20	0.0714
1	1/6	2.68 x 10^{-3}	32	0.114
0	0	0	36	0.129
-1	3/63	2.68 x 10^{-3}	32	0.114
-2	1/63	5.36 x 10^{-3}	20	0.0714

Table 5.2
Zeeman splitting for the *s* transitions ($M_1 \neq M_2$):

M_1	M_2	$g_1M_1 - g_2M_2$	½ $\Delta\lambda$ (Å) ½	I (K)	w
3	2	1	1.61 x 10^{-2}	30	0.107
2	1	7/6	1.88 x 10^{-2}	20	0.0714
1	0	4/3	2.15 x 10^{-2}	12	0.0429
0	1	3/2	2.42 x 10^{-2}	6	0.0214
-1	-2	5/3	2.68 x 10^{-2}	2	0.0071

+ 5 symmetric components

Thus, for this 587 nm transition, the effective Zeeman broadening for a 1 kGauss magnetic field is according to equation (1.23):

$$\gamma \approx 0.3651 \ \text{GHz} \bullet (\text{kGauss})^{-1} ,$$

α_D^{-1}, as given in equation (1.19), is:

$$\alpha_D^{1/2} \approx 11.82 \ \text{GHz} \bullet (\text{eV})^{-1/2}) .$$

Using equation (1.24), and noting that both terms are in GHz.

$$s_R = a_D^{1/2} T_i^{1/2} + g B = 11.82 \ T_i^{1/2} + 0.3651 \ B \qquad (\text{in GHz})$$

Note here that the Doppler term is much larger than the Zeeman term. This situation reflects the large Doppler Broadening associated with ion (or neutral) of small atomic mass. The expression is now ready to be used in equation (1.26) to extract the ion temperature (in eV). σFor an exact de-convolution, an approach similar to the one presented in section 4.2 can be used to obtain the helium neutral temperature.

6.0 REFERENCES

G. Herzberg, Atomic Spectra and Atomic Structure, Dover (1945)
G. Marr, Plasma Spectroscopy, Elsevier (1968)
H.R. Griem, Plasma Spectroscopy, McGraw-Hill (1964)
A. Corney, Atomic and Laser Spectroscopy, Clarendon Press (1977)
S. Bashkin and J.O. Stoner, Atomic Energy Levels and Grotrian Diagrams, N. Holland (1975)